

~~The dynamic~~ Dynamic stiffness matrix based on the extended separation-of-variables ~~type~~ solution for the free vibration of orthotropic rectangular thin plates

Shiyi Mei^a, Colin Caprani^{a,*}, Daniel Cantero^b

^a*Department of Civil Engineering, Monash University, Melbourne, Victoria, Australia*

^b*Department of Structural Engineering, Norwegian University of Science & Technology NTNU, Trondheim, Norway*

Abstract

The dynamic stiffness matrix (DSM) based on the extended separation-of-variables (SOV) ~~type-mode~~ solution is developed for the free vibration analysis of an orthotropic rectangular thin plate with general homogeneous boundary conditions. The method combines the advantages of the DSM method and the SOV method. The SOV ~~type~~ solution satisfies the governing differential equation derived from Rayleigh's principle and is used to formulate ~~the~~ dynamic stiffness matrices. Owing to the characteristics of the SOV ~~type~~ solution, the fully clamped boundary condition problem associated with the Wittrick–Williams algorithm is resolved. The enhanced algorithm is further proposed to solve dynamic stiffness matrices, rather than solving eigenvalue equations. A numerical technique for mode shape computation is also introduced. The accuracy of the proposed method is validated through numerical experiments.

1. Introduction

Rectangular plates play an important role in various engineering fields, including civil, mechanical, and aerospace engineering [3]. The free vibration of plates has been a fundamental research problem for over two centuries.

*Corresponding author

Email addresses: shiyi.mei1@monash.edu (Shiyi Mei), colin.caprani@monash.edu (Colin Caprani), daniel.cantero@ntnu.no (Daniel Cantero)

5 The earliest exact solutions for this problem are the Navier [21] and Levy
6 [14] solutions, which require at least one pair of opposite edges to be simply
7 supported or guided. To solve problems with other boundary conditions, ap-
8 proximate solutions such as the Rayleigh–Ritz method [13] and the Galerkin
9 method [12] have been widely applied. For these approximation methods,
10 beam functions, polynomials, trigonometric functions, and their combina-
11 tions [16] are commonly used as the assumed approximate functions. The
12 accuracy of these solutions depends on how well the assumed approximate
13 functions represent the displacement of the plate.

14 Besides the approximation methods, several analytical methods have been
15 developed over ~~the~~ past decades, including the Kantorovich-Krylov method
16 [9, 10], the symplectic eigenfunction expansion method [32, 25], the separation-
17 of-variable (SOV) method [29], the dynamic stiffness matrix (DSM) method
18 [2], and series expansion-based methods [24]. The series expansion-based
19 methods include the superposition method [22, 7], Fourier series method
20 [11, 17], the finite integral transform method [15, 33], and other series meth-
21 ods. These methods represent the plate displacement in terms of an infinite
22 series and mostly are capable of handling any general boundary conditions.
23 However, sufficient truncation of the series is required to ensure the accuracy
24 and convergence of the results, and the eigenvalue equation is generally dif-
25 ficult to express explicitly. Therefore, solving the corresponding eigenvalue
26 problem can be computationally expensive.

27 Despite being a powerful method for the dynamic analysis of plate as-
28 semblies, the finite element method (FEM) requires a sufficient number of
29 elements and is computationally expensive to accurately capture higher-order
30 modes. Thus, the DSM method was developed as an accurate and efficient
31 analytical approach to alternatively solve complex plate structures [4, 5]. The
32 DSM can be considered as an analytical FEM since the mode functions of
33 the plate are expressed by analytical solutions, where Levy-type solution [6]
34 or components of infinite Fourier series [1, 19] are applied. To avoid solving
35 the cumbersome transcendental frequency equation directly, the Wittrick-
36 Williams (W-W) algorithm [23] is applied to the eigenvalue problem. The
37 W-W algorithm determines the lower and upper bounds of natural frequen-
38 cies to arbitrary precision rather than solving the frequency equation directly.
39 Thus, the DSM has the potential to be effectively and systematically solved
40 using the W-W algorithm. However, a critical part in applying the W-W
41 algorithm is to ~~priorly~~ determine all natural frequencies of the fully clamped
42 structure within the interested frequency range, a priori. Strategies such as

using a sufficiently fine mesh or including a sufficient number of terms in series expansions [1] can ensure that all fully clamped frequencies are accounted for, thereby maintaining the accuracy of the algorithm. However, these approaches are computationally expensive and complex, posing a significant obstacle to the wider adoption and application of the DSM method based on the W-W algorithm [8]. To resolve the fully clamped plate problem, Liu and Banerjee [18] suggested that the frequencies can be indirectly obtained from the simply supported plate problem, where the Navier solution serves as the analytical solution. This provides a significant enhancement to the W-W algorithm, increasing the efficiency of applying DSM methods. However, the solutions are not explicit and closed-form, but are expressed in an infinite series form, where a sufficient number of truncation terms is required to ensure accuracy.

Inspired by the Navier and Levy solutions, Xing and Liu [29] proposed the SOV method, which provides concise and explicit eigensolutions. The mode shape function has a separable form, $\phi(x)\psi(y)$, requiring only one $\phi(x)$ and one $\psi(y)$ for each mode order, allowing each eigenvalue equation to be explicitly expressed. However, this SOV method is not suitable to deal with plates with free boundary conditions. Therefore, an extended SOV method [26, 27] based on the Rayleigh quotient was proposed to accommodate plates with all four classical boundary conditions, i.e., simply supported, clamped, guided, and free. Based on the Rayleigh quotient model, alternative iterative and improved SOV methods have been subsequently proposed [28]. Although SOV methods provide concise closed-form analytical solutions, they require solving a specific set of highly nonlinear eigenvalue equations for each type of boundary condition. However, even when considering only the four classic homogeneous cases, it becomes evident that 55 different boundary condition combinations exist for a rectangular plate, making the process tedious.

In this study, the SOV method is further extended to analyze the vibrations of plates with elastically restrained edges. ~~The extended SOV type~~ This extended SOV solution is then employed to construct ~~the~~ dynamic stiffness matrices, which accommodate all general homogeneous boundary conditions. By taking advantage of both the SOV and DSM methods, an enhanced W-W algorithm is developed to solve the eigenvalue problem without directly solving the eigenvalue equations. This enhanced approach resolves the challenge of determining fully clamped frequencies, a well-known limitation in the application of the W-W algorithm. In addition, a novel numerical technique ~~has been~~ is proposed to compute the mode shape coefficients.

81 2. Mathematical model

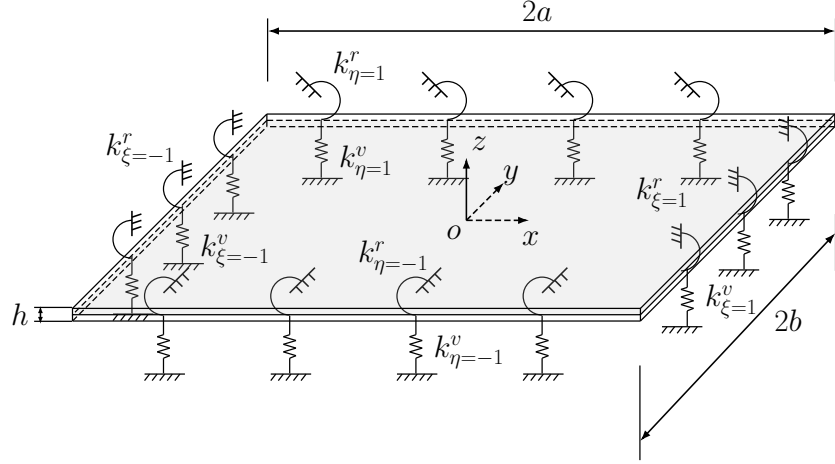


Figure 1: The orthotropic rectangular plate with all edges elastically restrained.

82 Consider a thin orthotropic rectangular plate of length $2a$ and width
 83 $2b$, with all four edges restrained by vertical translational springs k^v and
 84 rotational springs k^r , as shown in Figure 1. The coordinate origin is located
 85 at the center of the plate.

86 The governing differential equation for the free vibration of a thin or-
 87 thotropic plate is given by [28]:

$$D_{11} \frac{\partial^4 w}{\partial \xi^4} + 2D_3 \alpha \chi^2 \frac{\partial^4 w}{\partial \xi^2 \partial \eta^2} + D_{22} \alpha \chi^4 \frac{\partial^4 w}{\partial \eta^4} = \rho h \alpha h g^4 \omega^2 w, \quad (1)$$

88 where $\alpha = a/b$, $\chi = a/b$ is the aspect ratio; $\xi = x/a$ and $\eta = y/b$ are the
 89 normalized coordinates, and the bending stiffness parameters are defined as:

$$\begin{aligned} D_{11} &= \frac{E_1 h^3}{12(1 - v_{12}v_{21})}, & D_{22} &= \frac{E_2 h^3}{12(1 - v_{12}v_{21})}, \\ D_{66} &= \frac{G_{12} h^3}{12}, & D_{12} &= v_{12}D_{22} = v_{21}D_{11}, & D_3 &= D_{12} + 2D_{66}, \end{aligned} \quad (2)$$

90 where ρ and h denote the mass density and thickness of the plate, respec-
 91 tively; E_1 and E_2 are the Young's moduli in the x - and y -directions, respec-
 92 tively; G_{12} is the shear modulus, and v_{12} and v_{21} are the Poisson's ratios.

93 Instead of solving the free vibration of the thin orthotropic plate using
 94 Equation (1), it is suggested that the vibration of the thin plate can also be
 95 solved using the Rayleigh quotient variational principle [26]:

$$\delta U_{\text{mag}} = \underline{\omega}^2 \delta T_{\underline{0}}, \quad (3)$$

96 where δ denotes variation, $\underline{U_{\text{mag}}}$ is the magnitude of the potential energy
 97 of the plate, and $\underline{\omega^2 T_0}$ represents the magnitude of the kinetic energy of
 98 the plate. The potential energy of the plate can be expressed as [27]:

$$U^I = \frac{1}{2} \iint \left[D_{11} \left(\frac{\partial^2 W}{\partial x^2} \right)^2 + 2D_{12} \frac{\partial^2 W}{\partial x^2} \frac{\partial^2 W}{\partial y^2} + D_{22} \left(\frac{\partial^2 W}{\partial y^2} \right)^2 + 4D_{66} \left(\frac{\partial^2 W}{\partial x \partial y} \right)^2 \right] dx dy. \quad (4)$$

99 And the kinetic energy is:

$$T = \frac{1}{2} \iint \rho h \left(\frac{\partial W}{\partial t} \right)^2 dx dy. \quad (5)$$

100 Assuming the solution of the deflection $W(x, y; t) = w(x, y)e^{i\omega t}$ for har-
 101 monic plate motion, where $i = \sqrt{-1}$, $w(x, y)$ is the mode shape, and ω is the
 102 radial frequency. By substituting $W(x, y; t) = w(x, y)e^{i\omega t}$ into Equations (4)
 103 and (5) and expressing the system in dimensionless coordinates, we have:

$$U_{\text{mag}}^I = \frac{ab}{2} \iint \left[\frac{D_{11}}{a^4} \left(\frac{\partial^2 w}{\partial \xi^2} \right)^2 + \frac{2D_{12}}{a^2 b^2} \frac{\partial^2 w}{\partial \xi^2} \frac{\partial^2 w}{\partial \eta^2} + \frac{D_{22}}{b^4} \left(\frac{\partial^2 w}{\partial \eta^2} \right)^2 + \frac{4D_{66}}{a^2 b^2} \left(\frac{\partial^2 w}{\partial \xi \partial \eta} \right)^2 \right] d\xi d\eta, \quad (6)$$

104 and

$$T = \omega^2 \frac{ab}{2} \rho h \iint w^2 d\xi d\eta = \omega^2 T_0, \quad (7)$$

105 where, T_0 is defined as the coefficient of the kinetic energy.

106 The separable form of the mode shape function $w(\xi, \eta)$ is given by:

$$w(\xi, \eta) = \phi(\xi)\psi(\eta), \quad (8)$$

107 where $\phi(\xi)$ and $\psi(\eta)$ can be expressed as:

$$\phi(\xi) = A_1 \sin(\alpha_1 \xi) + A_2 \cos(\alpha_1 \xi) + A_3 \sinh(\beta_1 \xi) + A_4 \cosh(\beta_1 \xi), \quad (9a)$$

$$\psi(\eta) = B_1 \sin(\alpha_2 \eta) + B_2 \cos(\alpha_2 \eta) + B_3 \sinh(\beta_2 \eta) + B_4 \cosh(\beta_2 \eta). \quad (9b)$$

108 Based on Equation (3), the frequencies ω_x and ω_y , corresponding to the
 109 mode shapes $\phi(\xi)$ and $\psi(\eta)$, respectively, are assumed to be independent of
 110 each other. This is a common and important assumption in SOV methods,
 111 and ω_x and ω_y can be different in a mathematical sense [27].

112 2.1. Dynamic stiffness matrix corresponding to ω_x

113 For given general homogeneous boundary conditions, we can first assume
 114 that the mode shape $\psi(\eta)$ corresponding to the y -direction is known. Sup-
 115 posing the edges of the plate in both the x - and y -directions are elastically
 116 restrained by homogeneous vertical translational and rotational springs. The
 117 vertical translational and rotational springs at the $\xi = -1$ end are **defined**
 118 denoted as $k_{\xi=-1}^v$ and $k_{\xi=-1}^r$, respectively, and at the $\xi = 1$ end as $k_{\xi=1}^v$ and
 119 $k_{\xi=1}^r$, respectively. Thus, the potential energy along the supported edge in
 120 the x -direction can be expressed by:

$$\begin{aligned} U_{\sim}^{IIx} = & \int \left[k_{\xi=-1}^r \left(\frac{\partial W}{\partial x} \right)^2 + k_{\xi=-1}^v (W)^2 \right]_{x=-a} dy \\ & + \int \left[k_{\xi=1}^r \left(\frac{\partial W}{\partial x} \right)^2 + k_{\xi=1}^v (W)^2 \right]_{x=a} dy. \end{aligned} \quad (10)$$

121 From Equation (10), the magnitude of **total** potential energy along the plate
 122 edges in the x -direction, expressed in dimensionless coordinates, is obtained
 123 as:

$$\begin{aligned} U_{\sim}^{IIx} = & ab \int \left[\frac{k_{\xi=-1}^r}{a^3} \left(\frac{\partial w}{\partial \xi} \right)^2 + \frac{k_{\xi=-1}^v}{a} (w)^2 \right]_{\xi=-1} d\eta \\ & + ab \int \left[\frac{k_{\xi=1}^r}{a^3} \left(\frac{\partial w}{\partial \xi} \right)^2 + \frac{k_{\xi=1}^v}{a} (w)^2 \right]_{\xi=1} d\eta. \end{aligned} \quad (11)$$

124 The magnitude of total potential energy of the plate in the x -direction can
 125 be obtained from Equations (6) and (11) as:

$$\begin{aligned}
 U_{\underline{mag}} &= U^I_{\underline{mag}} + U^{II}_{\underline{mag}} \quad \text{with } x \text{ direction} \\
 &= \frac{ab}{2} \iint \left[\frac{D_{11}}{a^4} \left(\frac{\partial^2 w}{\partial \xi^2} \right)^2 + \frac{2D_{12}}{a^2 b^2} \frac{\partial^2 w}{\partial \xi^2} \frac{\partial^2 w}{\partial \eta^2} + \frac{D_{22}}{b^4} \left(\frac{\partial^2 w}{\partial \eta^2} \right)^2 \right. \\
 &\quad \left. + \frac{4D_{66}}{a^2 b^2} \left(\frac{\partial^2 w}{\partial \xi \partial \eta} \right)^2 \right] d\xi d\eta \\
 &\quad + ab \int \left[\frac{k_{\xi=1}^r}{a^3} \left(\frac{\partial w}{\partial \xi} \right)^2 + \frac{k_{\xi=1}^v}{a} (w)^2 \right]_{\xi=1} d\eta \\
 &\quad + ab \int \left[\frac{k_{\xi=-1}^r}{a^3} \left(\frac{\partial w}{\partial \xi} \right)^2 + \frac{k_{\xi=-1}^v}{a} (w)^2 \right]_{\xi=-1} d\eta
 \end{aligned} \tag{12}$$

126 By substituting Equation (8) into Equation (12), we have:

$$\begin{aligned}
 U_{\underline{mag}} &= U^I_{\underline{mag}} + U^{II}_{\underline{mag}} \equiv \frac{ab}{2} \int_{-1}^1 \left[\frac{D_{11}}{a^4} I_1 \left(\frac{d^2 \phi}{d\xi^2} \right)^2 + \frac{2D_{12}}{a^2 b^2} I_2 \frac{d^2 \phi}{d\xi^2} \phi + \frac{D_{22}}{b^4} I_4 \phi^2 \right. \\
 &\quad \left. + \frac{4D_{66}}{a^2 b^2} I_3 \left(\frac{d\phi}{d\xi} \right)^2 \right] d\xi \\
 &\quad + ab I_1 \left[\frac{k_{\xi=-1}^r}{a^3} \left(\frac{d\phi}{d\xi} \right)^2 + \frac{k_{\xi=-1}^v}{a} (\phi)^2 \right]_{\xi=-1} \\
 &\quad + ab I_1 \left[\frac{k_{\xi=1}^r}{a^3} \left(\frac{d\phi}{d\xi} \right)^2 + \frac{k_{\xi=1}^v}{a} (\phi)^2 \right]_{\xi=1},
 \end{aligned} \tag{13}$$

127 where the integral parameters ~~are defined as:-~~

$$\begin{aligned} I_1 &= \int_{-1}^1 \psi^2 d\eta, \\ I_2 &= \int_{-1}^1 \left(\frac{d^2\psi}{d\eta^2} \psi \right) d\eta, \\ I_3 &= \int_{-1}^1 \left(\frac{d\psi}{d\eta} \right)^2 d\eta, \\ I_4 &= \int_{-1}^1 \left(\frac{d^2\psi}{d\eta^2} \right)^2 d\eta. \end{aligned}$$

128 I_1, I_2, I_3 and I_4 are defined and expressed in Appendix A.

129 By taking Equation (8) into account, the coefficient T_0 of the kinetic
130 energy from Equation (7) for the plate in the x -direction can be expressed
131 as:

$$T_0 = \frac{ab}{2} \rho h \iint w^2 d\xi d\eta = \frac{ab}{2} \rho h I_1 \int_{-1}^1 \phi^2 d\xi. \quad (14)$$

132 ~~Take-~~

133 Taking the Rayleigh principle in the form:

$$\delta U_{\underline{mag}} = \omega_x^2 \delta T_{0.}, \quad (15)$$

134 ~~By and by~~ substituting Equations (13) and (14) into Equation (15), and re-
135 lieving $\delta\phi$ and $\delta \frac{d\phi}{d\xi}$ in Equation (15) by ~~variation calculus~~ calculus of variations,

136 yields:

$$\begin{aligned}
0 = & \int_{-1}^1 \left[\frac{D_{11}}{a^4} I_1 \frac{d^4 \phi}{d\xi^4} + \left(\frac{2D_{12}}{a^2 b^2} I_2 - \frac{4D_{66}}{a^2 b^2} I_3 \right) \frac{d^2 \phi}{d\xi^2} \right. \\
& + \left(\frac{D_{22}}{b^4} I_4 - \omega_x^2 \rho h I_1 \right) \phi \Big] \delta \phi d\xi \\
& + \frac{2k_{\xi=-1}^v}{a} I_1 (\phi \delta \phi)_{\xi=-1} + \frac{2k_{\xi=1}^v}{a} I_1 (\phi \delta \phi)_{\xi=1} \\
& + \left[\left(\frac{4D_{66}}{a^2 b^2} I_3 - \frac{D_{12}}{a^2 b^2} I_2 \right) \frac{d\phi}{d\xi} - \frac{D_{11}}{a^4} I_1 \frac{d^3 \phi}{d\xi^3} \right] \delta \phi \Big|_{\xi=-1}^{\xi=1} \\
& + \left(\frac{D_{12}}{a^2 b^2} I_2 \phi + \frac{D_{11}}{a^4} I_1 \frac{d^2 \phi}{d\xi^2} \right) \delta \frac{d\phi}{d\xi} \Big|_{\xi=-1}^{\xi=1} \\
& + \frac{2k_{\xi=-1}^r}{a^3} I_1 \left(\frac{d\phi}{d\xi} \delta \frac{d\phi}{d\xi} \right)_{\xi=-1} + \frac{2k_{\xi=1}^r}{a^3} I_1 \left(\frac{d\phi}{d\xi} \delta \frac{d\phi}{d\xi} \right)_{\xi=1}.
\end{aligned} \tag{16}$$

137 Thus, the governing differential equation in the x -direction can be obtained
138 from the integration part in Equation (16):

$$\frac{d^4 \phi}{d\xi^4} + 2\alpha\chi^2 \left(\frac{D_{12}I_2}{D_{11}I_1} - 2\frac{D_{66}I_3}{D_{11}I_1} \right) \frac{d^2 \phi}{d\xi^2} + \left(\frac{\alpha\chi^4}{D_{11}I_1} \frac{D_{22}I_4}{D_{11}I_1} - a^4 \Omega_x^4 \right) \phi = 0, \tag{17}$$

139 where $\Omega_x = \sqrt[4]{\omega_x^2 \rho h / D_{11}}$. By substituting $\phi(\xi) = Ae^{\mu\xi}$ into Equation (17),
140 yields we obtain:

$$\mu^4 + 2\alpha\chi^2 \left(\frac{D_{12}I_2}{D_{11}I_1} - 2\frac{D_{66}I_3}{D_{11}I_1} \right) \mu^2 + \left(\frac{\alpha\chi^4}{D_{11}I_1} \frac{D_{22}I_4}{D_{11}I_1} - a^4 \Omega_x^4 \right) = 0. \tag{18}$$

141 The And so the solution for μ can be expressed as:

$$\mu_{1,2} = \pm i\alpha_1, \quad \mu_{3,4} = \pm \beta_1, \tag{19}$$

142 where,

$$\alpha_1 = \alpha\chi \sqrt{\sqrt{\left(\frac{D_{12}I_2}{D_{11}I_1} - 2\frac{D_{66}I_3}{D_{11}I_1} \right)^2 - \frac{D_{22}I_4}{D_{11}I_1} + b^4 \Omega_x^4} + \frac{D_{12}I_2}{D_{11}I_1} - 2\frac{D_{66}I_3}{D_{11}I_1}}, \tag{20a}$$

$$\beta_1 = \alpha\chi \sqrt{\sqrt{\left(\frac{D_{12}I_2}{D_{11}I_1} - 2\frac{D_{66}I_3}{D_{11}I_1} \right)^2 - \frac{D_{22}I_4}{D_{11}I_1} + b^4 \Omega_x^4} - \frac{D_{12}I_2}{D_{11}I_1} + 2\frac{D_{66}I_3}{D_{11}I_1}}. \tag{20b}$$

143 The boundary conditions along the edges in the x -direction can be obtained
 144 from the remaining $\delta\phi$ and $\delta\frac{d\phi}{d\xi}$ parts in Equation (16). The shear force
 145 equilibrium can be obtained from the $\delta\phi$ part:

$$\begin{aligned} & \left[\left(\frac{4D_{66}}{a^2b^2} I_3 - \frac{D_{12}}{a^2b^2} I_2 \right) \frac{d\phi}{d\xi} - \frac{D_{11}}{a^4} I_1 \frac{d^3\phi}{d\xi^3} \right] \Big|_{\xi=-1}^{\xi=1} \\ & + \frac{2k_{\xi=-1}^v}{a} I_1 (\phi)_{\xi=-1} + \frac{2k_{\xi=1}^v}{a} I_1 (\phi)_{\xi=1} = 0, \end{aligned} \quad (21)$$

146 and from the $\delta\frac{d\phi}{d\xi}$ part, the bending moment equilibrium:

$$\begin{aligned} & \left(\frac{D_{12}}{a^2b^2} I_2 \phi + \frac{D_{11}}{a^4} I_1 \frac{\partial^2 \phi}{\partial \xi^2} \right) \Big|_{\xi=-1}^{\xi=1} \\ & + \frac{2k_{\xi=-1}^r}{a^3} I_1 \left(\frac{\partial \phi}{\partial \xi} \right)_{\xi=-1} - \frac{2k_{\xi=1}^r}{a^3} I_1 \left(\frac{\partial \phi}{\partial \xi} \right)_{\xi=1} = 0. \end{aligned} \quad (22)$$

147 Thus, we can obtain the shear force and bending moment equilibrium along
 148 the edges $\xi = -1$ and $\xi = 1$ from Equations (21) and (22), respectively, as:

$$\frac{d^3\phi}{d\xi^3} - \frac{\alpha\chi^2}{D_{11}I_1} \left(\frac{4D_{66}I_3}{D_{11}I_1} - \frac{D_{12}I_2}{D_{11}I_1} \right) \frac{d\phi}{d\xi} + \frac{2a^3k_{\xi=-1}^v}{D_{11}} \phi = 0, \quad \xi = -1, \quad (23a)$$

$$\frac{d^2\phi}{d\xi^2} + \frac{\alpha^2 D_{12} I_2}{D_{11} I_1} \frac{\chi^2 D_{12} I_2}{D_{11} I_1} \phi - \frac{2ak_{\xi=-1}^r}{D_{11}} \frac{d\phi}{d\xi} = 0, \quad \xi = -1, \quad (23b)$$

$$\frac{d^3\phi}{d\xi^3} - \frac{\alpha\chi^2}{D_{11}I_1} \left(\frac{4D_{66}I_3}{D_{11}I_1} - \frac{D_{12}I_2}{D_{11}I_1} \right) \frac{d\phi}{d\xi} - \frac{2a^3k_{\xi=1}^v}{D_{11}} \phi = 0, \quad \xi = 1, \quad (23c)$$

$$\frac{d^2\phi}{d\xi^2} + \frac{\alpha^2 D_{12} I_2}{D_{11} I_1} \frac{\chi^2 D_{12} I_2}{D_{11} I_1} \phi + \frac{2ak_{\xi=1}^r}{D_{11}} \frac{d\phi}{d\xi} = 0, \quad \xi = 1. \quad (23d)$$

149 Substituting Equation (9a) into Equation (23), and denoting $k_{\xi}^{v*} = \frac{2a^3k_{\xi}^v}{D_{11}}$,
 150 $k_{\xi}^{r*} = \frac{2ak_{\xi}^r}{D_{11}}$, $S_{\alpha_1} = \sin \alpha_1$, $C_{\alpha_1} = \cos \alpha_1$, $Sh_{\alpha_1} = \sinh \alpha_1$, $Ch_{\alpha_1} = \cosh \alpha_1$, $k_{\xi}^{v*} = \frac{2a^3k_{\xi}^v}{D_{11}}$,
 151 $k_{\eta}^{r*} = \frac{2ak_{\eta}^r}{D_{11}}$, $S_{\alpha_1} = \sin \alpha_1$, $C_{\alpha_1} = \cos \alpha_1$, $Sh_{\beta_1} = \sinh \beta_1$, and $Ch_{\beta_1} = \cosh \beta_1$,

152 ~~$S_{\beta_1} = \sin \beta_1$, $C_{\beta_1} = \cos \beta_1$, $Sh_{\beta_1} = \sinh \beta_1$, and $Ch_{\beta_1} = \cosh \beta_1$~~ , we have:

$$\begin{bmatrix} \gamma_1 C_{\alpha_1} - k_{\xi=-1}^{v*} S_{\alpha_1} & \gamma_1 S_{\alpha_1} + k_{\xi=-1}^{v*} C_{\alpha_1} & \gamma_2 Ch_{\beta_1} - k_{\xi=-1}^{v*} Sh_{\beta_1} \\ \gamma_3 S_{\alpha_1} + k_{\xi=-1}^{r*} \alpha_1 C_{\alpha_1} & -\gamma_3 C_{\alpha_1} + k_{\xi=-1}^{r*} \alpha_1 S_{\alpha_1} & \gamma_4 Sh_{\beta_1} + k_{\xi=-1}^{r*} \beta_1 Ch_{\beta_1} \\ -\gamma_1 C_{\alpha_1} + k_{\xi=1}^{v*} S_{\alpha_1} & \gamma_1 S_{\alpha_1} + k_{\xi=1}^{v*} C_{\alpha_1} & -\gamma_2 Ch_{\beta_1} + k_{\xi=1}^{v*} Sh_{\beta_1} \\ \gamma_3 S_{\alpha_1} + k_{\xi=1}^{r*} \alpha_1 C_{\alpha_1} & \gamma_3 C_{\alpha_1} - k_{\xi=1}^{r*} \alpha_1 S_{\alpha_1} & \gamma_4 Sh_{\beta_1} + k_{\xi=1}^{r*} \beta_1 Ch_{\beta_1} \\ -\gamma_2 Sh_{\beta_1} + k_{\xi=-1}^{v*} Ch_{\beta_1} & & \\ -\gamma_4 Ch_{\beta_1} - k_{\xi=-1}^{r*} \beta_1 Sh_{\beta_1} & & \\ -\gamma_2 Sh_{\beta_1} + k_{\xi=1}^{v*} Ch_{\beta_1} & & \\ \gamma_4 Ch_{\beta_1} + k_{\xi=1}^{r*} \beta_1 Sh_{\beta_1} & & \end{bmatrix} \begin{Bmatrix} A_1 \\ A_2 \\ A_3 \\ A_4 \end{Bmatrix} = \begin{Bmatrix} 0 \\ 0 \\ 0 \\ 0 \end{Bmatrix}, \quad (24)$$

153 or,

$$\mathbf{R}_x \mathbf{A} = \mathbf{0}, \quad (25)$$

154 where,

$$\begin{aligned} \gamma_1 &= -\alpha_1^3 - \alpha \chi^2 \left(\frac{4D_{66}S_3}{D_{11}I_1} - \frac{D_{12}I_2}{D_{11}I_1} \right) \alpha_1, \\ \gamma_2 &= \beta_1^3 - \alpha \chi^2 \left(\frac{4D_{66}S_3}{D_{11}I_1} - \frac{D_{12}I_2}{D_{11}I_1} \right) \beta_1, \\ \gamma_3 &= -\alpha_1^2 + \frac{\alpha^2 D_{12}I_2}{D_{11}I_1} \frac{\chi^2 D_{12}I_2}{\underbrace{D_{11}I_1}}, \\ \gamma_4 &= \beta_1^2 + \frac{\alpha^2 D_{12}I_2}{D_{11}I_1} \frac{\chi^2 D_{12}I_2}{\underbrace{D_{11}I_1}}. \end{aligned} \quad (26)$$

155 Note that the classic boundary conditions can be obtained by selecting ex-
 156 tremely large or small spring stiffness constants. For non-trivial solutions,
 157 the characteristic equation or eigenvalue equation is obtained from the de-
 158 terminant of the matrix \mathbf{R}_x in Equation (25), which must be zero. How-
 159 ever, solving these transcendental equations ~~are cumbersome and tedious;~~
 160 ~~thus is cumbersome and so~~ the DSM is ~~introduced to avoid the ineffective~~
 161 ~~introduced to avoid such a~~ computation.

162 To develop ~~its the plate's~~ dynamic stiffness matrix, with the help of Equa-
 163 tion (9a), the vertical displacement and rotation corresponding to the mode
 164 shape $\phi(\xi)$ along the x -direction at edges $\xi = -1$ and $\xi = 1$ can be expressed

165 as:

$$\begin{Bmatrix} \phi_{\xi=-1} \\ \frac{d\phi}{d\xi}_{\xi=-1} \\ \phi_{\xi=1} \\ \frac{d\phi}{d\xi}_{\xi=1} \end{Bmatrix} = \begin{bmatrix} -S_{\alpha_1} & C_{\alpha_1} & -Sh_{\beta_1} & Ch_{\beta_1} \\ \alpha_1 C_{\alpha_1}/a & \alpha_1 S_{\alpha_1}/a & \beta_1 Ch_{\beta_1}/a & -\beta_1 Sh_{\beta_1}/a \\ S_{\alpha_1} & C_{\alpha_1} & Sh_{\beta_1} & Ch_{\beta_1} \\ \alpha_1 C_{\alpha_1}/a & -\alpha_1 S_{\alpha_1}/a & \beta_1 Ch_{\beta_1}/a & \beta_1 Sh_{\beta_1}/a \end{bmatrix} \begin{Bmatrix} A_1 \\ A_2 \\ A_3 \\ A_4 \end{Bmatrix}, \quad (27)$$

166 or,

$$\delta_x = \mathbf{Q}_x \mathbf{A}. \quad (28)$$

167 ~~Note that Solving for~~ the eigenvector \mathbf{A} ~~can be expressed by multiplying the~~
 168 ~~inverse matrix \mathbf{Q}_x^{-1} on the left side of Equation (28), and then substituting~~
 169 ~~\mathbf{A} into Equation (25), we obtain:~~

$$\mathbf{R}_x \mathbf{A} = \mathbf{R}_x \mathbf{Q}_x^{-1} \delta_x = \mathbf{0}. \quad (29)$$

170 where the dynamic stiffness matrix, denoted as $\mathbf{K}_x = \mathbf{R}_x \mathbf{Q}_x^{-1}$, can be ob-
 171 tained from Equation (29). This matrix can be used to compute the natural
 172 frequencies of the system instead of solving the eigenvalue equation, and the
 173 method for the computation will be given in Section 3.

174 2.2. Dynamic stiffness matrix corresponding to ω_y

175 In this section, the mode shape $\phi(\xi)$ derived in *Section 2.1* is utilized to
 176 obtain the dynamic stiffness matrix in the y -direction. The vertical trans-
 177 lational and rotational springs at $\eta = -1$ are denoted as $k_{\eta=-1}^v$ and $k_{\eta=-1}^r$,
 178 respectively, while those at $\eta = 1$ are represented by $k_{\eta=1}^v$ and $k_{\eta=1}^r$.

179 ~~The magnitude of total potential energy along the edges in the y -direction~~
 180 ~~is given by:-~~

$$\begin{aligned} \underline{U_{mag}^{III}} = & \underline{ab \int \left[\frac{k_{\eta=-1}^r}{a^3} \left(\frac{\partial w}{\partial \eta} \right)^2 + \frac{k_{\eta=-1}^v}{a} w^2 \right]_{\eta=-1} d\xi} \\ & + ab \int \left[\frac{k_{\eta=1}^r}{a^3} \left(\frac{\partial w}{\partial \eta} \right)^2 + \frac{k_{\eta=1}^v}{a} w^2 \right]_{\eta=1} d\xi. \end{aligned}$$

181 ~~The Following the same steps as for the x-direction, the~~ magnitude of poten-
 182 ~~tial energy of the plate in the y -direction can be obtained from Equation (6) and section 2.2-~~

183 as:

$$\begin{aligned}
 U_{\underline{mag}} = \underline{U_{mag}^I} + \underline{U_{mag}^{III}} &= \frac{ab}{2} \int_{-1}^1 \left[\frac{D_{11}}{a^4} \frac{\partial^2 w}{\partial \xi^2} \underline{J_4} \psi^2 + \frac{2D_{12}}{a^2 b^2} \frac{\partial^2 w}{\partial \xi^2} \frac{\partial^2 w}{\partial \eta^2} \frac{2D_{12}}{a^2 b^2} J_2 \frac{d^2 \psi}{d\eta^2} \psi + \frac{D_{22}}{b^4} J_1 \left(\frac{\partial^2 w}{\partial \eta^2} \frac{d^2 \psi}{d\eta^2} \right)^2 \right. \\
 &+ \left. \frac{4D_{66}}{a^2 b^2} \frac{4D_{66}}{a^2 b^2} J_3 \left(\frac{\partial^2 w}{\partial \xi \partial \eta} \frac{d\psi}{d\eta} \right)^2 \right] d\underline{\xi} \eta + \underline{ab} \int \underline{ab} J_1 \left[\frac{k_{\eta=1}^r}{b^3} \left(\frac{\partial w}{\partial \eta} \frac{d\psi}{d\eta} \right)^2 + \frac{k_{\eta=1}^v}{b} \left(\underline{w\psi} \right)^2 \right]_{\eta=1} \underline{\xi} \\
 &+ \underline{ab} \int \underline{ab} J_1 \left[\frac{k_{\eta=-1}^r}{b^3} \left(\frac{\partial w}{\partial \eta} \frac{d\psi}{d\eta} \right)^2 + \frac{k_{\eta=-1}^v}{b} \left(\underline{w\psi} \right)^2 \right]_{\eta=-1} \underline{\xi}, \tag{30}
 \end{aligned}$$

184 By substituting Equation (8) into ??, we obtain:-

$$\begin{aligned}
 \underline{U_{mag}} &= \underline{U_{mag}^I} + \underline{U_{mag}^{III}} \\
 &= \frac{ab}{2} \int_{-1}^1 \left[\frac{D_{11}}{a^4} J_4 \psi^2 + \frac{2D_{12}}{a^2 b^2} J_2 \frac{d^2 \psi}{d\eta^2} \psi + \frac{D_{22}}{b^4} J_1 \left(\frac{d^2 \psi}{d\eta^2} \right)^2 \right. \\
 &\quad \left. + \frac{4D_{66}}{a^2 b^2} J_3 \left(\frac{d\psi}{d\eta} \right)^2 \right] d\eta + ab J_1 \left[\frac{k_{\eta=1}^r}{b^3} \left(\frac{d\psi}{d\eta} \right)^2 + \frac{k_{\eta=1}^v}{b} (\psi)^2 \right]_{\eta=1} \\
 &\quad + ab J_1 \left[\frac{k_{\eta=-1}^r}{b^3} \left(\frac{d\psi}{d\eta} \right)^2 + \frac{k_{\eta=-1}^v}{b} (\psi)^2 \right]_{\eta=-1},
 \end{aligned}$$

185 where the integral parameters are defined as:-

$$\begin{aligned}
 \underline{J_1} &= \int_{-1}^1 \phi^2 d\xi, \\
 \underline{J_2} &= \int_{-1}^1 \left(\frac{d^2 \phi}{d\xi^2} \phi \right) d\xi, \\
 \underline{J_3} &= \int_{-1}^1 \left(\frac{d\phi}{d\xi} \right)^2 d\xi, \\
 \underline{J_4} &= \int_{-1}^1 \left(\frac{d^2 \phi}{d\xi^2} \right)^2 d\xi.
 \end{aligned}$$

186 J_1, J_2, J_3 , and J_4 are defined and expressed in Appendix A.

187 The coefficient T_0 of the kinetic energy from Equation (7) for the plate
188 in the y -direction can be expressed as:

$$T_0 = \frac{ab}{2} \rho h J_1 \int_{-1}^1 \psi^2 d\eta. \quad (31)$$

189 Take the Rayleigh principle in the form:

$$\delta U_{\text{mag}} = \omega_y^2 \delta T_0. \quad (32)$$

190 By substituting Section 2.2 and equation (31) into Equation (32), and relieving $\delta\psi$ and $\delta \frac{d\psi}{d\eta}$ in Equation (32) by ~~variation calculus~~ calculus of variation,
191 yields:
192

$$\begin{aligned} 0 = & \int_{-1}^1 \left[\frac{D_{22}}{b^4} J_1 \frac{d^4\psi}{d\eta^4} + \left(\frac{2D_{12}}{a^2b^2} J_2 - \frac{4D_{66}}{a^2b^2} J_3 \right) \frac{d^2\psi}{d\eta^2} \right. \\ & + \left(\frac{D_{11}}{a^4} J_4 - \omega_y^2 \rho h J_1 \right) \psi \Big] \delta\psi d\eta \\ & + \frac{2k_{\eta=-1}^v}{b} J_1 (\psi \delta\psi)_{\eta=-1} + \frac{2k_{\eta=1}^v}{b} J_1 (\psi \delta\psi)_{\eta=1} \\ & + \left[\left(\frac{4D_{66}}{a^2b^2} J_3 - \frac{D_{12}}{a^2b^2} J_2 \right) \frac{d\psi}{d\eta} - \frac{D_{22}}{b^4} J_1 \frac{d^3\psi}{d\eta^3} \right] \delta\psi \Big|_{\eta=-1}^{\eta=1} \\ & + \left(\frac{D_{12}}{a^2b^2} J_2 \psi + \frac{D_{22}}{b^4} J_1 \frac{d^2\psi}{d\eta^2} \right) \delta \frac{d\psi}{d\eta} \Big|_{\eta=-1}^{\eta=1} \\ & + \frac{2k_{\eta=-1}^r}{b^3} J_1 \left(\frac{d\psi}{d\eta} \delta \frac{d\psi}{d\eta} \right)_{\eta=-1} + \frac{2k_{\eta=1}^r}{b^3} J_1 \left(\frac{d\psi}{d\eta} \delta \frac{d\psi}{d\eta} \right)_{\eta=1}. \end{aligned} \quad (33)$$

193 Thus, the governing differential equation in the y -direction can be obtained
194 from the integration part in Equation (33):

$$\frac{d^4\psi}{d\eta^4} + \frac{\textcolor{red}{2}}{\textcolor{red}{\alpha}^2} \frac{\textcolor{blue}{2}}{\textcolor{blue}{\chi}^2} \left(\frac{D_{12}J_2}{D_{22}J_1} - 2 \frac{D_{66}J_3}{D_{22}J_1} \right) \frac{d^2\psi}{d\eta^2} + \left(\frac{\textcolor{red}{D_{11}J_4}}{\textcolor{red}{\alpha}^4 \textcolor{red}{D_{22}J_1}} \frac{\textcolor{blue}{D_{11}J_4}}{\textcolor{blue}{\chi}^4 \textcolor{blue}{D_{22}J_1}} - \frac{b^4 D_{11}}{D_{22}} \Omega_y^4 \right) \psi = 0, \quad (34)$$

195 where $\Omega_y = \sqrt[4]{\omega_y^2 \rho h / D_{11}}$. By substituting $\psi(\eta) = B e^{\lambda \eta}$ into Equation (34),
196 yields:

$$\lambda^4 + \frac{\textcolor{red}{2}}{\textcolor{red}{\alpha}^2} \frac{\textcolor{blue}{2}}{\textcolor{blue}{\chi}^2} \left(\frac{D_{12}J_2}{D_{22}J_1} - 2 \frac{D_{66}J_3}{D_{22}J_1} \right) \lambda^2 + \left(\frac{\textcolor{red}{D_{11}J_4}}{\textcolor{red}{\alpha}^4 \textcolor{red}{D_{22}J_1}} \frac{\textcolor{blue}{D_{11}J_4}}{\textcolor{blue}{\chi}^4 \textcolor{blue}{D_{22}J_1}} - \frac{b^4 D_{11}}{D_{22}} \Omega_y^4 \right) = 0. \quad (35)$$

197 The solution for λ can be expressed as:

$$\lambda_{1,2} = \pm i\alpha_2, \quad \lambda_{3,4} = \pm \beta_2, \quad (36)$$

198 where,

$$\alpha_2 = \frac{1}{\alpha} \frac{1}{\lambda} \sqrt{\left(\frac{D_{12}J_2}{D_{22}J_1} - 2 \frac{D_{66}J_3}{D_{22}J_1} \right)^2 - \frac{D_{11}J_4}{D_{22}J_1} + \frac{a^4 D_{11}}{D_{22}} \Omega_y^4 + \frac{D_{12}J_2}{D_{22}J_1} - 2 \frac{D_{66}J_3}{D_{22}J_1}}, \quad (37a)$$

$$\beta_2 = \frac{1}{\alpha} \frac{1}{\lambda} \sqrt{\left(\frac{D_{12}J_2}{D_{22}J_1} - 2 \frac{D_{66}J_3}{D_{22}J_1} \right)^2 - \frac{D_{11}J_4}{D_{22}J_1} + \frac{a^4 D_{11}}{D_{22}} \Omega_y^4 - \frac{D_{12}J_2}{D_{22}J_1} + 2 \frac{D_{66}J_3}{D_{22}J_1}}. \quad (37b)$$

199 The boundary conditions along the edges in the y -direction can be obtained
 200 from the remaining $\delta\psi$ and $\delta \frac{d\psi}{d\eta}$ parts in Equation (33). The shear force
 201 equilibrium can be obtained from the $\delta\psi$ part:

$$\left[\left(\frac{4D_{66}}{a^2b^2} J_3 - \frac{D_{12}}{a^2b^2} J_2 \right) \frac{d\psi}{d\eta} - \frac{D_{22}}{b^4} J_1 \frac{d^3\psi}{d\eta^3} \right] \Big|_{\eta=-1}^{\eta=1} + \frac{2k_{\eta=-1}^v}{b} J_1(\psi)_{\eta=-1} + \frac{2k_{\eta=1}^v}{b} J_1(\psi)_{\eta=1} = 0, \quad (38)$$

202 and from the $\delta \frac{d\psi}{d\eta}$ part, the bending moment equilibrium:

$$\left(\frac{D_{12}}{a^2b^2} J_2 \psi + \frac{D_{22}}{b^4} J_1 \frac{d^2\psi}{d\eta^2} \right) \Big|_{\eta=-1}^{\eta=1} + \frac{2k_{\eta=-1}^r}{b^3} J_1 \left(\frac{d\psi}{d\eta} \right)_{\eta=-1} + \frac{2k_{\eta=1}^r}{b^3} J_1 \left(\frac{d\psi}{d\eta} \right)_{\eta=1} = 0. \quad (39)$$

203 ~~Thus, we can obtain~~ Similarly, from the shear force and bending moment
 204 ~~equilibrium along the edges $\eta = -1$, and $\eta = 1$ from Equations (38) and (39)~~

205 ~~, respectively, as:~~

$$\begin{aligned}
& \frac{d^3\psi}{d\eta^3} - \left(\frac{4D_{66}J_3}{\alpha^2 D_{22}J_1} - \frac{D_{12}J_2}{\alpha^2 D_{22}J_1} \right) \frac{d\psi}{d\eta} + \frac{2b^3 k_{\eta=-1}^v}{D_{22}} \psi = 0, & \underline{\eta = -1}, \\
& \frac{d^2\psi}{d\eta^2} + \frac{D_{12}J_2}{\alpha^2 D_{22}J_1} \psi - \frac{2b k_{\eta=-1}^r}{D_{22}} \frac{d\psi}{d\eta} = 0, & \underline{\eta = -1}, \\
& \frac{d^3\psi}{d\eta^3} - \left(\frac{4D_{66}J_3}{\alpha^2 D_{22}J_1} - \frac{D_{12}J_2}{\alpha^2 D_{22}J_1} \right) \frac{d\psi}{d\eta} - \frac{2b^3 k_{\eta=1}^v}{D_{22}} \psi = 0, & \underline{\eta = 1}, \\
& \frac{d^2\psi}{d\eta^2} + \frac{D_{12}J_2}{\alpha^2 D_{22}J_1} \psi + \frac{2b k_{\eta=1}^r}{D_{22}} \frac{d\psi}{d\eta} = 0, & \underline{\eta = 1}.
\end{aligned}$$

206 ~~Substituting Equation (9b) into ?? and~~ by denoting $k_{\eta}^{v*} = \frac{2b^3 k_{\eta}^v}{D_{22}}$, $k_{\eta}^{r*} = \frac{2b k_{\eta}^r}{D_{22}}$,
207 $S_{\alpha_2} = \sin \alpha_2$, $C_{\alpha_2} = \cos \alpha_2$, ~~$Sh_{\alpha_2} = \sinh \alpha_2$, $Ch_{\alpha_2} = \cosh \alpha_2$, $S_{\beta_2} = \sin \beta_2$,~~
208 ~~$C_{\beta_2} = \cos \beta_2$, $Sh_{\beta_2} = \sinh \beta_2$, and $Ch_{\beta_2} = \cosh \beta_2$~~ , We can obtain:

$$\begin{aligned}
& \begin{bmatrix} \zeta_1 C_{\alpha_2} - k_{\eta=-1}^{v*} S_{\alpha_2} & \zeta_1 S_{\alpha_2} + k_{\eta=-1}^{v*} C_{\alpha_2} & \zeta_2 Ch_{\beta_2} - k_{\eta=-1}^{v*} Sh_{\beta_2} \\ \zeta_3 S_{\alpha_2} + k_{\eta=-1}^{r*} \alpha_2 C_{\alpha_2} & -\zeta_3 C_{\alpha_2} + k_{\eta=-1}^{r*} \alpha_2 S_{\alpha_2} & \zeta_4 Sh_{\beta_2} + k_{\eta=-1}^{r*} \beta_2 Ch_{\beta_2} \\ -\zeta_1 C_{\alpha_2} + k_{\eta=1}^{v*} S_{\alpha_2} & \zeta_1 S_{\alpha_2} + k_{\eta=1}^{v*} C_{\alpha_2} & -\zeta_2 Ch_{\beta_2} + k_{\eta=1}^{v*} Sh_{\beta_2} \\ \zeta_3 S_{\alpha_2} + k_{\eta=1}^{r*} \alpha_2 C_{\alpha_2} & \zeta_3 C_{\alpha_2} - k_{\eta=1}^{r*} \alpha_2 S_{\alpha_2} & \zeta_4 Sh_{\beta_2} + k_{\eta=1}^{r*} \beta_2 Ch_{\beta_2} \\ -\zeta_2 Sh_{\beta_2} + k_{\eta=-1}^{v*} Ch_{\beta_2} \\ -\zeta_4 Ch_{\beta_2} - k_{\eta=-1}^{r*} \beta_2 Sh_{\beta_2} \\ -\zeta_2 Sh_{\beta_2} + k_{\eta=1}^{v*} Ch_{\beta_2} \\ \zeta_4 Ch_{\beta_2} + k_{\eta=1}^{r*} \beta_2 Sh_{\beta_2} \end{bmatrix} \begin{Bmatrix} B_1 \\ B_2 \\ B_3 \\ B_4 \end{Bmatrix} = \begin{Bmatrix} 0 \\ 0 \\ 0 \\ 0 \end{Bmatrix}, \\
& \hspace{25em} (40)
\end{aligned}$$

209 OR,

$$\mathbf{R}_y \mathbf{B} = \mathbf{0}, \tag{41}$$

210 where,

$$\begin{aligned}
\zeta_1 &= -\alpha_2^3 - \left(\frac{4D_{66}J_3}{\alpha^2 D_{22}J_1} \frac{4D_{66}J_3}{\chi^2 D_{22}J_1} - \frac{D_{12}J_2}{\alpha^2 D_{22}J_1} \frac{D_{12}J_2}{\chi^2 D_{22}J_1} \right) \alpha_2, \\
\zeta_2 &= \beta_2^3 - \left(\frac{4D_{66}T_3}{\alpha^2 D_{22}J_1} \frac{4D_{66}T_3}{\chi^2 D_{22}J_1} - \frac{D_{12}J_2}{\alpha^2 D_{22}J_1} \frac{D_{12}J_2}{\chi^2 D_{22}J_1} \right) \beta_2, \\
\zeta_3 &= -\alpha_2^2 + \frac{D_{12}J_2}{\alpha^2 D_{22}J_1} \frac{D_{12}J_2}{\chi^2 D_{22}J_1}, \\
\zeta_4 &= \beta_2^2 + \frac{D_{12}J_2}{\alpha^2 D_{22}J_1} \frac{D_{12}J_2}{\chi^2 D_{22}J_1}.
\end{aligned} \tag{42}$$

211 With the help of Equation (9b), the vertical displacement and rotation cor-
 212 responding to the mode shape ψ along the y -direction at the edges $\eta = -1$
 213 and $\eta = 1$ can be expressed as:

$$\begin{Bmatrix} \psi_{\eta=-1} \\ \frac{d\psi}{d\eta}_{\eta=-1} \\ \psi_{\eta=1} \\ \frac{d\psi}{d\eta}_{\eta=1} \end{Bmatrix} = \begin{bmatrix} -S_{\alpha_2} & C_{\alpha_2} & -Sh_{\beta_2} & Ch_{\beta_2} \\ \alpha_2 C_{\alpha_2}/b & \alpha_2 S_{\alpha_2}/b & \beta_2 Ch_{\beta_2}/b & -\beta_2 Sh_{\beta_2}/b \\ S_{\alpha_2} & C_{\alpha_2} & Sh_{\beta_2} & Ch_{\beta_2} \\ \alpha_2 C_{\alpha_2}/b & -\frac{\alpha_2 S_{\alpha_2}}{b} & \beta_2 Ch_{\beta_2}/b & \beta_2 Sh_{\beta_2}/b \end{bmatrix} \begin{Bmatrix} B_1 \\ B_2 \\ B_3 \\ B_4 \end{Bmatrix}, \tag{43}$$

214 or,

$$\delta_y = \mathbf{Q}_y \mathbf{B}. \tag{44}$$

215 ~~Note that Solving for the eigenvector \mathbf{B} can be expressed by multiplying the~~
 216 ~~inverse matrix \mathbf{Q}_y^{-1} on the left-hand side of Equation (44), and then substituting \mathbf{B} into Equation (41), we obtain:~~

$$\mathbf{R}_y \mathbf{B} = \mathbf{R}_y \mathbf{Q}_y^{-1} \delta_y = \mathbf{0}, \tag{45}$$

218 where the dynamic stiffness matrix, denoted as $\mathbf{K}_y = \mathbf{R}_y \mathbf{Q}_y^{-1}$, can be ob-
 219 tained from Equation (45).

220 3. Frequency and mode shape computation

221 3.1. Wittrick-Williams algorithm and enhancement

222 The Wittrick-Williams (W-W) algorithm [23] is an effective method for
 223 determining the natural frequencies from the dynamic stiffness matrix with

high reliability. Instead of directly solving the equations, the algorithm computes the total number J of natural frequencies below a given frequency ω^* , which is represented as:

$$J(\omega^*) = J_0(\omega^*) + s\{\mathbf{K}^\Delta(\omega^*)\} = J_0(\omega^*) + J_k(\omega^*), \quad (46)$$

where J_0 represents the number of natural frequencies of the structure with all ends fully clamped, \mathbf{K}^Δ is the upper triangular matrix obtained from the dynamic stiffness matrix \mathbf{K} after applying Gaussian elimination, and $J_k(\omega^*)$ denotes the number of negative elements in the leading diagonal of \mathbf{K}^Δ .

It should be noted that the J_0 count is a crucial aspect when applying the W-W algorithm. Many previous studies use a sufficiently fine mesh or enough terms in series expansions to capture all fully clamped natural frequencies, ensuring computational accuracy [1]. However, this approach can make the application process cumbersome. To address this issue, the fully clamped problem can be replaced with a simply supported problem, where the Navier solution for the simply supported plate is used to count J_0 [18]. Nevertheless, since analytical solutions in DSM methods involve an infinite series of Fourier terms, a sufficient number of truncation terms is required to ensure accuracy and convergence.

In fact, J_0 can be indirectly determined by evaluating the number of natural frequencies J of the structure under specific boundary conditions, which are generally different from the original boundary conditions [8]:

$$J_0(p_1, \omega^*) = J(\bar{p}_1, \omega^*) - J_k(\bar{p}_1, \omega^*), \quad (47)$$

where p_1 denotes the fully clamped supports, and \bar{p}_1 denotes specific supports, which are typically simply supported, guided, or a combination of the two. For these specific boundary conditions, the eigenvalue equations of SOV type solution take the form of a single harmonic function. By substituting Equation (47) into Equation (46) we get the algorithm as:

$$J(p, \omega^*) = J(\bar{p}_1, \omega^*) - J_k(\bar{p}_1, \omega^*) + J_k(p, \omega^*) \quad (48)$$

where p represents the original boundary conditions of the structure. Therefore, the challenge of determining $J_0(p_1, \omega^*)$ can be transformed into the problem of solving $J(\bar{p}_1, \omega^*)$ instead. ~~By considering~~

By taking fully simply supported boundary conditions as the example, the eigenvalue equation corresponding to the natural frequency parameter

254 Ω_x can be obtained from the determinant of the coefficient matrix \mathbf{R}_x in
 255 Equation (24), as given by:

$$\sin 2\alpha_1 = 0. \quad (49)$$

256 With the help of Equations (20a) and (49), the closed-form solution of the
 257 n_x -th simply supported frequency Ω_{x,n_x} for the given n_y -order $\psi_{n_y}(\eta)$ can be
 258 expressed as:

$$\frac{1}{b} \sqrt[4]{\left[\left(\frac{n_x \pi}{2\alpha} \right)^2 - \frac{D_{12}S_2}{D_{11}S_1} + 2 \frac{D_{66}S_3}{D_{11}S_1} \right]^2 - \left(\frac{D_{12}S_2}{D_{11}S_1} - 2 \frac{D_{66}S_3}{D_{11}S_1} \right)^2 + \frac{D_{22}S_4}{D_{11}S_1}} b \Omega_{x,n_x}^4 = \left[\left(\frac{n_x \pi}{2\chi} \right)^2 - \frac{D_{12}S_2}{D_{11}S_1} + 2 \frac{D_{66}S_3}{D_{11}S_1} \right]^2 - \left(\frac{D_{12}S_2}{D_{11}S_1} - 2 \frac{D_{66}S_3}{D_{11}S_1} \right)^2 + \frac{D_{22}S_4}{D_{11}S_1}. \quad (50)$$

259 For $\Omega_{x,n_x} \leq \Omega_x^* < \Omega_{x,n_x+1}$, $J(\bar{p}_1, \Omega_x^*) = n_x$. Similarly, the closed-form
 260 solution of the n_y -th simply supported frequency Ω_{y,n_y} for the given n_x -order
 261 $\phi_{n_x}(\xi)$ can be expressed as:

$$\frac{1}{a} \sqrt[4]{\frac{D_{22}}{D_{11}} \left\{ \left[\left(\frac{n_y \pi \alpha}{2} \right)^2 - \frac{D_{12}T_2}{D_{22}T_1} + 2 \frac{D_{66}T_3}{D_{22}T_1} \right]^2 - \left(\frac{D_{12}T_2}{D_{22}T_1} - 2 \frac{D_{66}T_3}{D_{22}T_1} \right)^2 + \frac{D_{11}T_4}{D_{22}T_1} \right\}} a \Omega_{y,n_y}^4 = \frac{D_{22}}{D_{11}} \left\{ \left[\left(\frac{n_y \pi \alpha}{2} \right)^2 - \frac{D_{12}T_2}{D_{22}T_1} + 2 \frac{D_{66}T_3}{D_{22}T_1} \right]^2 - \left(\frac{D_{12}T_2}{D_{22}T_1} - 2 \frac{D_{66}T_3}{D_{22}T_1} \right)^2 + \frac{D_{11}T_4}{D_{22}T_1} \right\}. \quad (51)$$

262 For $\Omega_{y,n_y} \leq \Omega_y^* < \Omega_{y,n_y+1}$, $J(\bar{p}_1, \Omega_y^*) = n_y$. According to the relationships
 263 $\Omega_x = \sqrt[4]{\omega_x^2 \rho h / D_{11}} \Omega_x^4 = \omega_x^2 \rho h / D_{11}$ and $\Omega_y = \sqrt[4]{\omega_y^2 \rho h / D_{11}} \Omega_y^4 = \omega_y^2 \rho h / D_{11}$, the
 264 values of $J(\bar{p}_1, \omega_x^*)$ and $J(\bar{p}_1, \omega_y^*)$ can be derived from $J(\bar{p}_1, \Omega_x^*)$ and $J(\bar{p}_1, \Omega_y^*)$,
 265 respectively. Therefore, this refined W-W algorithm can be applied to esti-
 266 mate the lower and upper bounds of the frequency range, denoted as ω_l and
 267 ω_u , yielding an approximation for the frequency $\omega_a \in (\omega_l, \omega_u)$ to arbitrary
 268 precision.

269 3.2. Mode shape computation

270 The mode shape coefficients A_1 to A_4 and B_1 to B_4 in the eigenvectors \mathbf{A}
 271 and \mathbf{B} for all classic boundary conditions are provided in [27]. Alternatively,
 272 these coefficients can also be obtained through a simple numerical method,
 273 which this work presents as an approach. Here, we illustrate solving the

274 eigenvector \mathbf{A} as an example. By assuming the exact natural frequency as
 275 ω_k , we can expand the coefficient matrix \mathbf{R}_x in Equation (24) using a first-
 276 order Taylor series about ω_a :

$$\mathbf{R}_{x,k}(\omega_k)\mathbf{A}_k = \mathbf{R}_{x,a}\mathbf{A}_k + (\omega_k - \omega_a)\mathbf{R}'_{x,a}\mathbf{A}_k + O((\omega_k - \omega_a)^2) = 0. \quad (52)$$

277 Ignoring higher-order terms, an eigenvalue problem can be derived from
 278 Equation (52):

$$(\mathbf{R}'_{x,a})^{-1}\mathbf{R}_{x,a}\mathbf{A} = (\omega_a - \omega_k)\mathbf{A} = \tau\mathbf{A}. \quad (53)$$

279 This eigenvalue problem can be solved using the inverse iteration procedure
 280 [30]:

$$\bar{\mathbf{A}}^{(i+1)} = \mathbf{R}_{x,a}^{-1}\mathbf{R}'_{x,a}\mathbf{A}^{(i)}, \quad (54)$$

281 where the initial guess for $\mathbf{A}^{(0)}$ is a column vector consisting of four randomly
 282 generated elements, each of which falls within the range (0,1). The updated
 283 eigenvalue for the next step can be obtained as:

$$\tau^{(i+1)} = \frac{1}{\bar{A}_j^{(i+1)}}, \quad (55)$$

284 where,

$$|\bar{A}_j^{(i+1)}| = \max(|\bar{A}_1^{(i+1)}|, |\bar{A}_2^{(i+1)}|, |\bar{A}_3^{(i+1)}|, |\bar{A}_4^{(i+1)}|). \quad (56)$$

285 The updated eigenvector can be obtained as:

$$\mathbf{A}^{(i+1)} = \tau^{(i+1)}\bar{\mathbf{A}}^{(i+1)}. \quad (57)$$

286 The procedure can be controlled by the error tolerance ϵ or maximum allowed
 287 steps i_{\max} :

$$\max |A_n^{(i+1)} - A_n^{(i)}| < \epsilon, \quad (58a)$$

$$i = i_{\max}. \quad (58b)$$

288 Note that the mode shape coefficients A_1 to A_4 obtained from $\mathbf{A}^{(i+1)}$ are
 289 applied for the elastically restrained boundary conditions.

290 3.3. Application procedure

291 The procedure of the proposed method is as follows:

- 292 • **Step 1** Assume initial integral parameters $I_1^{(0)}$, $I_2^{(0)}$, $I_3^{(0)}$, and $I_4^{(0)}$ in the
 293 y -direction. Using the given boundary conditions at $\xi = -1$ and $\xi = 1$,
 294 determine $\mathbf{K}_x^{(0)}$ from Equation (29). Then, apply the computational
 295 algorithms in Section 3.1 to compute the lower and upper bounds of the
 296 n_x -th non-dimensional frequency parameter, $2a\Omega_{l,x,n_x}^{(0)}$ and $2a\Omega_{u,x,n_x}^{(0)}$,
 297 and take the average $2a\Omega_{x,n_x}^{(0)} = (2a\Omega_{l,x,n_x}^{(0)} + 2a\Omega_{u,x,n_x}^{(0)})/2$ along with its
 298 corresponding mode shape $\phi_{n_x}^{(0)}$, where $n_x = 1, 2, 3, \dots$
- 299 • **Step 2** Use $\phi_{n_x}^{(0)}$ as the prescribed mode to determine $\mathbf{K}_y^{(1)}$ in Equa-
 300 tion (45), considering the boundary conditions at $\eta = -1$ and $\eta = 1$.
 301 Apply the computational algorithms to obtain the n_y -th frequency pa-
 302 rameter $2a\Omega_{y,n_y}^{(1)}$ and its corresponding mode shape $\psi_{n_y}^{(1)}$, where $n_y =$
 303 $1, 2, 3, \dots$. This completes the first iteration cycle.
- 304 • **Step 3** Use $\psi_{n_y}^{(1)}$ as the prescribed n_y -th mode shape in the y -direction to
 305 compute $\mathbf{K}_x^{(1)}$ from Equation (29), then determine the n_x -th frequency
 306 parameter $2a\Omega_{x,n_x}^{(1)}$ and its corresponding mode shape $\phi_{n_x}^{(1)}$.
- 307 • **Step 4** Use $\phi_{n_x}^{(1)}$ as the prescribed mode in the x -direction to com-
 308 pute the n_y -th frequency parameter $2a\Omega_{y,n_y}^{(2)}$ and its corresponding mode
 309 shape $\psi_{n_y}^{(2)}$, completing the second iteration cycle.
- 310 • **Step 5** Stop the iteration if $|2a\Omega_{x,n_x}^{(i)} - 2a\Omega_{x,n_x}^{(i+1)}| \leq \Delta 2a\Omega$ or $|2a\Omega_{y,n_y}^{(i)} -$
 311 $2a\Omega_{y,n_y}^{(i+1)}| \leq \Delta 2a\Omega$, where $\Delta 2a\Omega = 2a\Omega_u - 2a\Omega_l$. Here, $2a\Omega_l$ and $2a\Omega_u$
 312 are the lower and upper bounds of the frequency parameter range,
 313 within which the actual frequency parameter $2a\Omega$ lies, i.e., $2a\Omega \in$
 314 $(2a\Omega_l, 2a\Omega_u)$. The quantity $\Delta 2a\Omega$ represents the frequency param-
 315 eter interval used in the W-W algorithm.
- 316 • **Step 6** Finally, construct the (n_x, n_y) -th mode shape as $w(\xi, \eta) =$
 317 $\phi_{n_x}(\xi)\psi_{n_y}(\eta)$ using Equation (8).

318 4. Numerical Results

319 This section presents the numerical validation of the proposed method for
 320 classic boundary conditions and rotationally restrained boundary conditions.

For all numerical calculations, the initial integral parameters are assumed as $I_1^{(0)} = 1$, $I_2^{(0)} = 1$, $I_3^{(0)} = 1$, and $I_4^{(0)} = 10$ in the y -direction, serving as the starting point of **Step 1** for any mode in all boundary conditions. In this section, the interval between the upper and lower bounds of the non-dimensional frequency parameter, $2a\Delta\Omega$, is set to 0.005, ~~limiting the error range~~ although any desired level of precision can be used. According to our numerical calculations, two iteration cycles are generally sufficient to meet the convergence requirement (i.e., $|2a\Omega_x^{(i)} - 2a\Omega_x^{(i+1)}| \leq \Delta 2a\Omega$ or $|2a\Omega_y^{(i)} - 2a\Omega_y^{(i+1)}| \leq \Delta 2a\Omega$) for most cases, with at most three cycles required when applying the iterative procedure in Section 3.3.

4.1. Classical boundary conditions

In this subsection, the proposed method is validated by comparison with the extended SOV method [27]. The properties of the orthotropic plate, consistent with those in [27], are as follows: $E_1 = 185$ GPa, $E_2 = 10.5$ GPa, $G_{12} = 7.3$ GPa, $\rho = 1600$ kg m⁻³, and $\nu_{12} = 0.28$.

The translational springs ($k_\xi^v k_\xi^v$) and rotational springs ($k_\xi^r k_\xi^r$) along all edges can be set to zero or infinity (represented as 1×10^{15} N m⁻¹ in the numerical calculations of this study) to obtain different classic boundary conditions.

The results for SSSS, SCSF, GCGC, CCCC, SSCC, SCCC, GGCC, CCFF, CFCF, CFFF, and FFFF boundary conditions are presented in Tables 1 to 3. Note that, as is convention, S is a simple support (rotation, no translation), C is a clamped supported (no rotation or translation), G is a guided support (translation, no rotation), and F is a free edge. These results demonstrate high accuracy compared to the extended SOV method, with difference remaining smaller than the frequency parameter interval $2a\Delta\Omega = 0.005$. The frequency parameters in both directions are equal ($2a\Omega_x - 2a\Omega_y = 0$) in almost all cases, with a few exceptions where $2a\Omega_x - 2a\Omega_y = 0.005$. In fact, higher accuracy compared to the extended SOV method can be achieved if the frequency parameter interval $2a\Delta\Omega$ is set smaller than 0.005. It should be noted that the accuracy improves only by reducing $2a\Delta\Omega$, and no additional iterations are required according to our calculations. Figure 2 shows the first six nonzero mode shapes of a square orthotropic plate with FFFF boundary conditions, where the mode shape coefficients are calculated using the numerical method developed in this study. Instead of selecting fixed expressions for the mode shape coefficients based on specific boundary conditions, our method is applicable to all boundary conditions.

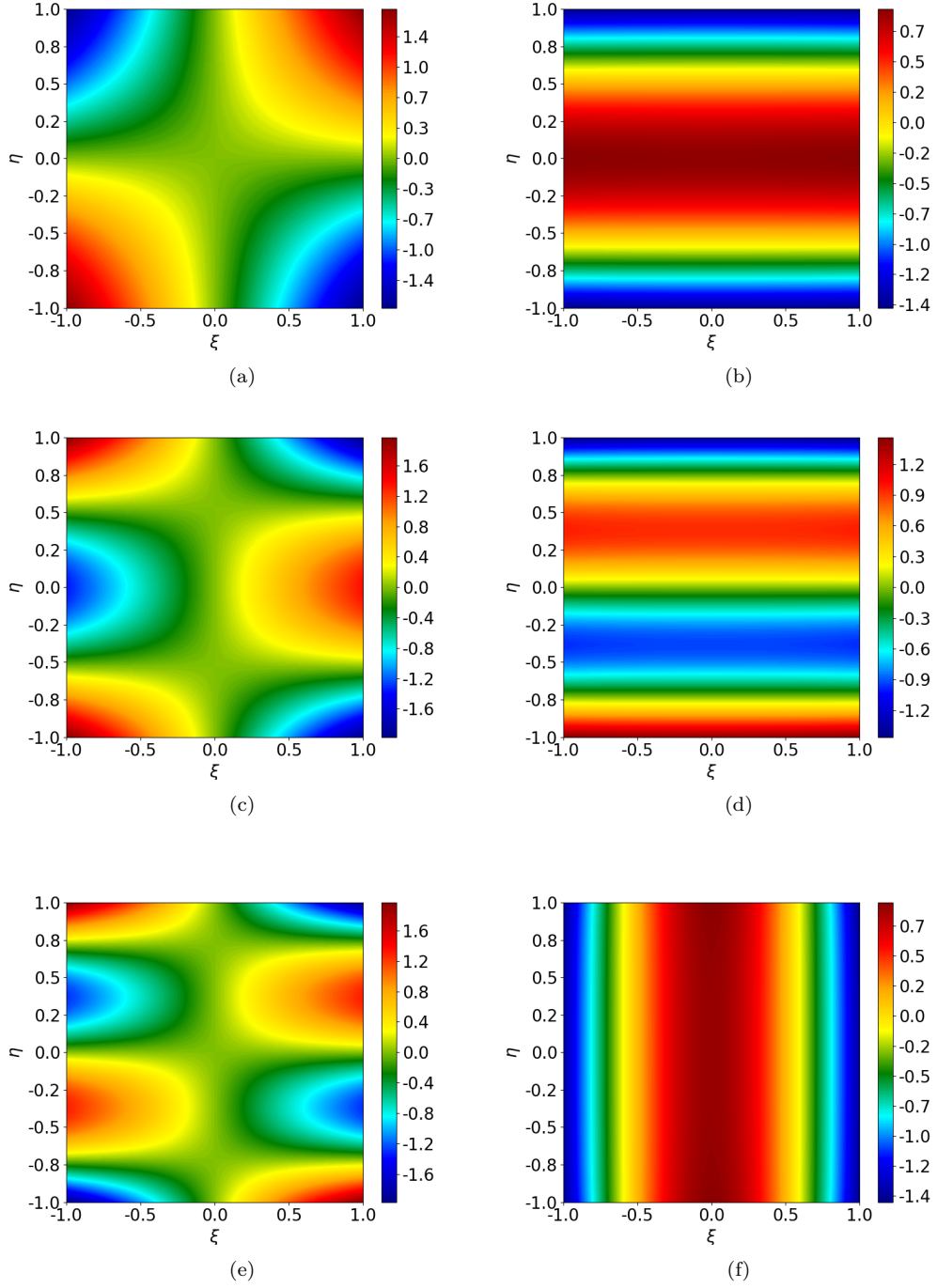


Figure 2: The first six nonzero mode shapes of a square orthotropic plate with FFFF boundary conditions: (a) the first mode; (b) the second mode; (c) the third mode; (d) the fourth mode; (e) the fifth mode; (f) the sixth mode.

Table 1: The first seven frequency parameter $2a\Omega$ of of orthotropic rectangular plates with SSSS, SCSF and GCGC boundary conditions.


BCs		Mode	$2a\Omega_x = 2a\Omega_y = 2a\sqrt[4]{\rho h \omega^2 / D_{11}}$						
			1	2	3	4	5	6	7
SSSS	0.5	Mode number	(1,1)	(1,2)	(1,3)	(1,4)	(1,5)	(1,6)	(1,7)
		extended SOV 27	3.1807	3.3190	3.5938	4.0135	4.5495	5.1635	5.8265
		Present	3.1825	3.3225	3.5975	4.0175	4.5525	5.1625	5.8275
	1	Mode number	(1,1)	(1,2)	(1,3)	(2,1)	(1,4)	(2,2)	(2,3)
		extended SOV 27	3.3190	4.0135	5.1635	6.3615	6.5200	6.6379	7.1876
		Present	3.3175	4.0175	5.1625	6.3625	6.5175	6.6375	7.1875
	1.5	Mode number	(1,1)	(1,2)	(2,1)	(2,2)	(1,3)	(2,3)	(1,4)
		extended SOV 27	3.5938	5.1635	6.4698	7.1876	7.2331	8.5389	9.4352
		Present	3.5975	5.1675	6.4725	7.1875	7.2325	8.5375	9.4375
SCSF	0.5	Mode number	(1,1)	(1,2)	(1,3)	(1,4)	(1,5)	(1,6)	(1,7)
		extended SOV 27	3.1516	3.2451	3.4588	3.8131	4.2950	4.8711	5.5087
		Present	3.1525	3.2475	3.4575	3.8175	4.2925	4.8725	5.5075
	1	Mode number	(1,1)	(1,2)	(1,3)	(1,4)	(2,1)	(2,2)	(2,3)
		extended SOV 27	3.1908	3.6428	4.5972	5.8599	6.3033	6.4901	6.9177
		Present	3.1925	3.6425	4.5975	5.8575	6.3025	6.4925	6.9175
	1.5	Mode number	(1,1)	(1,2)	(1,3)	(2,1)	(2,2)	(2,3)	(1,4)
		extended SOV 27	3.2710	4.3430	6.2157	6.3337	6.8043	7.8718	8.3518
		Present	3.2725	4.3425	6.2175	6.3325	6.8025	7.8725	8.3525
GCGC	0.5	Mode number	(1,1)	(1,2)	(1,3)	(2,1)	(2,2)	(1,4)	(2,3)
		extended SOV 27	1.1544	1.9166	2.6835	3.1983	3.3890	3.4501	3.7372
		Present	1.1525	1.9175	2.6825	3.1975	3.3875	3.4525	3.7375
	1	Mode number	(1,1)	(2,1)	(1,2)	(2,2)	(1,3)	(2,3)	(3,1)
		extended SOV 27	2.3087	3.4900	3.8331	4.4682	5.3669	5.7736	6.3967
		Present	2.3075	3.4875	3.8325	4.4675	5.3675	5.7725	6.3975
	1.5	Mode number	(1,1)	(2,1)	(1,2)	(2,2)	(3,1)	(3,2)	(1,3)
		extended SOV 27	3.4631	4.1353	5.7497	6.0981	6.6049	7.6449	8.0504
		Present	3.4625	4.1325	5.7475	6.0975	6.6075	7.6425	8.0525

Table 2: The first seven frequency parameter $2a\Omega$ of of orthotropic rectangular plates with CCCC, SSCC, SCCC and GGCC boundary conditions.


BCs		Mode	$2a\Omega_x = 2a\Omega_y = 2a\sqrt{\rho h \omega^2 / D_{11}}$						
			1	2	3	4	5	6	7
CCCC	0.5	Mode number	(1,1)	(1,2)	(1,3)	(1,4)	(1,5)	(1,6)	(1,7)
		extended SOV 27	4.7500	4.8208	4.9682	5.2177	5.5791	6.0430	6.5892
		Present	4.7475	4.8225	4.9725	5.2175	5.5825	6.0425	6.5875
	1	Mode number	(1,1)	(1,2)	(1,3)	(1,4)	(2,1)	(2,2)	(2,3)
		extended SOV 27	4.8579	5.3546	6.2819	7.4972	7.9193	8.1490	8.6054
		Present	4.8575	5.3575	6.2875	7.4975	7.9175	8.1475	8.6075
	1.5	Mode number	(1,1)	(1,2)	(2,1)	(1,3)	(2,2)	(2,3)	(1,4)
		extended SOV 27	5.1581	6.5412	8.0409	8.4945	8.7204	9.9793	10.6460
		Present	5.1575	6.5375	8.0425	8.4975	8.7175	9.9775	10.6425
SSCC	0.5	Mode number	(1,1)	(1,2)	(1,3)	(1,4)	(1,5)	(1,6)	(1,7)
		extended SOV 27	3.9542	4.0520	4.2525	4.5785	5.0254	5.5682	6.1789
		Present	3.9575	4.0525	4.2475	4.5775	5.0225	5.5725	6.1825
	1	Mode number	(1,1)	(1,2)	(1,3)	(1,4)	(2,1)	(2,2)	(2,3)
		extended SOV 27	4.0745	4.6606	5.7009	6.9940	7.1396	7.3894	7.8881
		Present	4.0775	4.6625	5.7025	6.9925	7.1375	7.3875	7.8875
	1.5	Mode number	(1,1)	(1,2)	(2,1)	(1,3)	(2,2)	(2,3)	(1,4)
		extended SOV 27	4.3602	5.8384	7.2531	7.8560	7.9481	9.2515	10.0366
		Present	4.3625	5.8325	7.2525	7.8575	7.9525	9.2525	10.0325
SCCC	0.5	Mode number	(1,1)	(1,2)	(1,3)	(1,4)	(1,5)	(1,6)	(1,7)
		extended SOV 27	3.9596	4.0745	4.3027	4.6606	5.1361	5.7009	6.3271
		Present	3.9575	4.0725	4.3025	4.6625	5.1325	5.7025	6.3325
	1	Mode number	(1,1)	(1,2)	(1,3)	(2,1)	(1,4)	(2,2)	(2,3)
		extended SOV 27	4.1349	4.8478	5.9805	7.1541	7.3192	7.4478	8.0121
		Present	4.1325	4.8475	5.9825	7.1525	7.3175	7.4475	8.0125
	1.5	Mode number	(1,1)	(1,2)	(2,1)	(2,2)	(1,3)	(2,3)	(3,1)
		extended SOV 27	4.5824	6.2766	7.3116	8.1528	8.3705	9.5986	10.3507
		Present	4.5825	6.2775	7.3125	8.1525	8.3725	9.5975	10.3525
GGCC	0.5	Mode number	(1,1)	(1,2)	(1,3)	(1,4)	(1,5)	(1,6)	(1,7)
		extended SOV 27	2.3750	2.4841	2.7895	3.2946	3.9226	4.6123	5.3326
		Present	2.3725	2.4875	2.7925	3.2975	3.9225	4.6075	5.3325
	1	Mode number	(1,1)	(1,2)	(1,3)	(2,1)	(2,2)	(1,4)	(2,3)
		extended SOV 27	2.4290	3.1410	4.4293	5.5202	5.7315	5.8801	6.2606
		Present	2.4325	3.1425	4.4325	5.5225	5.7325	5.8775	6.2625
	1.5	Mode number	(1,1)	(1,2)	(2,1)	(2,2)	(1,3)	(2,3)	(3,1)
		extended SOV 27	2.5790	4.2472	5.5565	6.1533	6.4347	7.5231	8.6732
		Present	2.5825	4.2475	5.5575	6.1525	6.4325	7.5225	8.6725

Table 3: The first seven nonzero frequency parameter $2a\Omega$ of of orthotropic rectangular plates with CCFF, CFCF, CFFF and FFFF boundary conditions.

BCs	α	χ	Mode	$2a\Omega_x = 2a\Omega_y = 2a\sqrt{\rho h \omega^2 / D_{11}}$						
				1	2	3	4	5	6	7
CCFF	0.5		Mode number	(1,1)	(1,2)	(1,3)	(1,4)	(1,5)	(1,6)	(2,1)
			extended SOV 27	1.8978	2.0905	2.4925	3.0563	3.7110	4.4117	4.7029
			Present	1.8975	2.0925	2.4925	3.0575	3.7125	4.4125	4.7025
	1		Mode number	(1,1)	(1,2)	(1,3)	(2,1)	(2,2)	(1,4)	(2,3)
			extended SOV 27	1.9930	2.7895	4.0733	4.7338	5.0652	5.5128	5.7419
			Present	1.9925	2.7875	4.0725	4.7325	5.0675	5.5125	5.7425
	1.5		Mode number	(1,1)	(1,2)	(2,1)	(2,2)	(1,3)	(2,3)	(3,1)
			extended SOV 27	2.1780	3.7411	4.7931	5.5758	5.8895	7.0263	7.9006
			Present	2.1775	3.7425	4.7925	5.5725	5.8875	7.0275	7.9025
CFCF	0.5		Mode number	(1,1)	(1,2)	(1,3)	(1,4)	(1,5)	(1,6)	(1,7)
			extended SOV 27	4.7297	4.7427	4.7881	4.8819	5.0478	5.3072	5.6694
			Present	4.7275	4.7425	4.7875	4.8825	5.0475	5.3075	5.6675
	1		Mode number	(1,1)	(1,2)	(1,3)	(1,4)	(1,5)	(1,6)	(2,1)
			extended SOV 27	4.7295	4.7817	5.0012	5.5348	6.4407	7.6182	7.8523
			Present	4.7275	4.7825	5.0025	5.5325	6.4425	7.6175	7.8525
	1.5		Mode number	(1,1)	(1,2)	(1,3)	(1,4)	(2,1)	(2,2)	(2,3)
			extended SOV 27	4.7292	4.8458	5.4221	6.7635	7.8518	7.9470	8.3021
			Present	4.7275	4.8475	5.4225	6.7625	7.8525	7.9475	8.3025
CFFF	0.5		Mode number	(1,1)	(1,2)	(1,3)	(1,4)	(1,5)	(1,6)	(1,7)
			extended SOV 27	1.8751	1.9439	2.1679	2.5657	3.1106	3.7486	4.4382
			Present	1.8775	1.9425	2.1675	2.5675	3.1125	3.7475	4.4375
	1		Mode number	(1,1)	(1,2)	(1,3)	(1,4)	(2,1)	(2,2)	(2,3)
			extended SOV 27	1.8750	2.1242	2.9077	4.1319	4.6937	4.8226	5.2263
			Present	1.8775	2.1225	2.9075	4.1325	4.6925	4.8225	5.2275
	1.5		Mode number	(1,1)	(1,2)	(1,3)	(2,1)	(2,2)	(2,3)	(1,4)
			extended SOV 27	1.8750	2.3402	3.8522	4.6935	4.9753	5.8314	5.9292
			Present	1.8775	2.3425	3.8525	4.6925	4.9775	5.8325	5.9275
FFFF	0.5		Mode number	(1,3)	(2,2)	(1,4)	(2,3)	(1,5)	(2,4)	(2,5)
			extended SOV 27	1.1540	1.4858	1.9157	2.1704	2.6821	2.7881	3.4093
			Present	1.1525	1.4875	1.9175	2.1725	2.6825	2.7875	3.4075
	1		Mode number	(2,2)	(1,3)	(2,3)	(1,4)	(2,4)	(3,1)	(3,2)
			extended SOV 27	2.1311	2.3082	3.2734	3.8320	4.4962	4.7298	4.9138
			Present	2.1325	2.3075	3.2725	3.8325	4.4975	4.7275	4.9125
	1.5		Mode number	(2,2)	(1,3)	(2,3)	(3,1)	(3,2)	(1,4)	(3,3)
			extended SOV 27	2.6277	3.4625	4.2915	4.7296	5.1259	5.7485	6.1588
			Present	2.6275	3.4625	4.2925	4.7275	5.1275	5.7475	6.1575

358 4.2. ~~Rotationally restrained boundary conditions~~ Rotational spring-supported
 359 edges

360 In this subsection, rectangular orthotropic plates with ~~rotationally restrained~~
 361 ~~edges~~ rotational spring-supported edges with no translations ($k_\xi^v = k_\eta^v = \infty$)
 362 are ~~validated~~ examined. The rotational stiffness coefficients are defined as:

$$r_\xi = \frac{2ak_\xi^r}{D_{11}}, \quad (59a)$$

$$r_\eta = \frac{2bk_\eta^r}{D_{22}}. \quad (59b)$$

363 The first example considers a square isotropic plate with all four edges ro-
 364 tationally restrained. The vertical translational springs along the four edges
 365 are numerically set as $k_{\xi=-1}^v = k_{\xi=1}^v = k_{\eta=-1}^v = k_{\eta=1}^v = 1 \times 10^{12} \text{ N m}^{-1}$. The
 366 material properties are given as $D_{11} = D_{22} = D_3$ and $\nu_{12} = \nu_{21} = 0.3$.

367 Table 4 presents the frequency parameter $2a\Omega$ for different rotational
 368 stiffness coefficients $r_\xi = r_\eta$ with values 0.1, 1, 10, 100, and 1000. Notably,
 369 when $r_\xi = r_\eta = 0$ and $r_\xi = r_\eta = \infty$, the boundary conditions correspond to
 370 SSSS and CCCC, respectively.

371 Interestingly, the results indicate that the frequencies Ω_x and Ω_y are
 372 not strictly equal for some mode shapes under ~~rotationally restrained~~ these
 373 boundary conditions. The actual frequency Ω lies between Ω_x and Ω_y , which
 374 may be attributed to the fact that Ω_x and Ω_y satisfy Rayleigh's principle in
 375 Equation (3), representing the weak-form governing equations, but do not
 376 necessarily satisfy the strong-form governing equations in Equation (1). For
 377 a physical problem with exact solutions, both Equations (1) and (3) must be
 378 satisfied. If this condition is not met, applying Equation (3) still provides a
 379 viable approach for approximating the exact solution of the plate. Thus, the
 380 exact frequency can be estimated as $\Omega = (\Omega_x + \Omega_y)/2$. As shown in Table 4,
 381 the maximum difference between Ω and the solutions reported in 31 is less
 382 than 1.3%. Figure 3 illustrates the variation in mode shapes corresponding
 383 to the fundamental natural frequency as the rotational stiffness $r_\xi = r_\eta$ in-
 384 creases from zero to ∞ , transitioning the boundary conditions from SSSS to
 385 CCCC.

386 The next example considers a rectangular orthotropic plate with three
 387 simply supported edges ($k_{\xi=-1}^r = k_{\xi=1}^r = k_{\eta=1}^r = 0$), while the edge at $\eta = -1$
 388 is rotationally restrained. The material properties are consistent with those
 389 in 31, where $2D_{11} = 2D_{22} = D_3$ and $\nu_{12} = \nu_{21} = 0.3$. Table 5 shows the

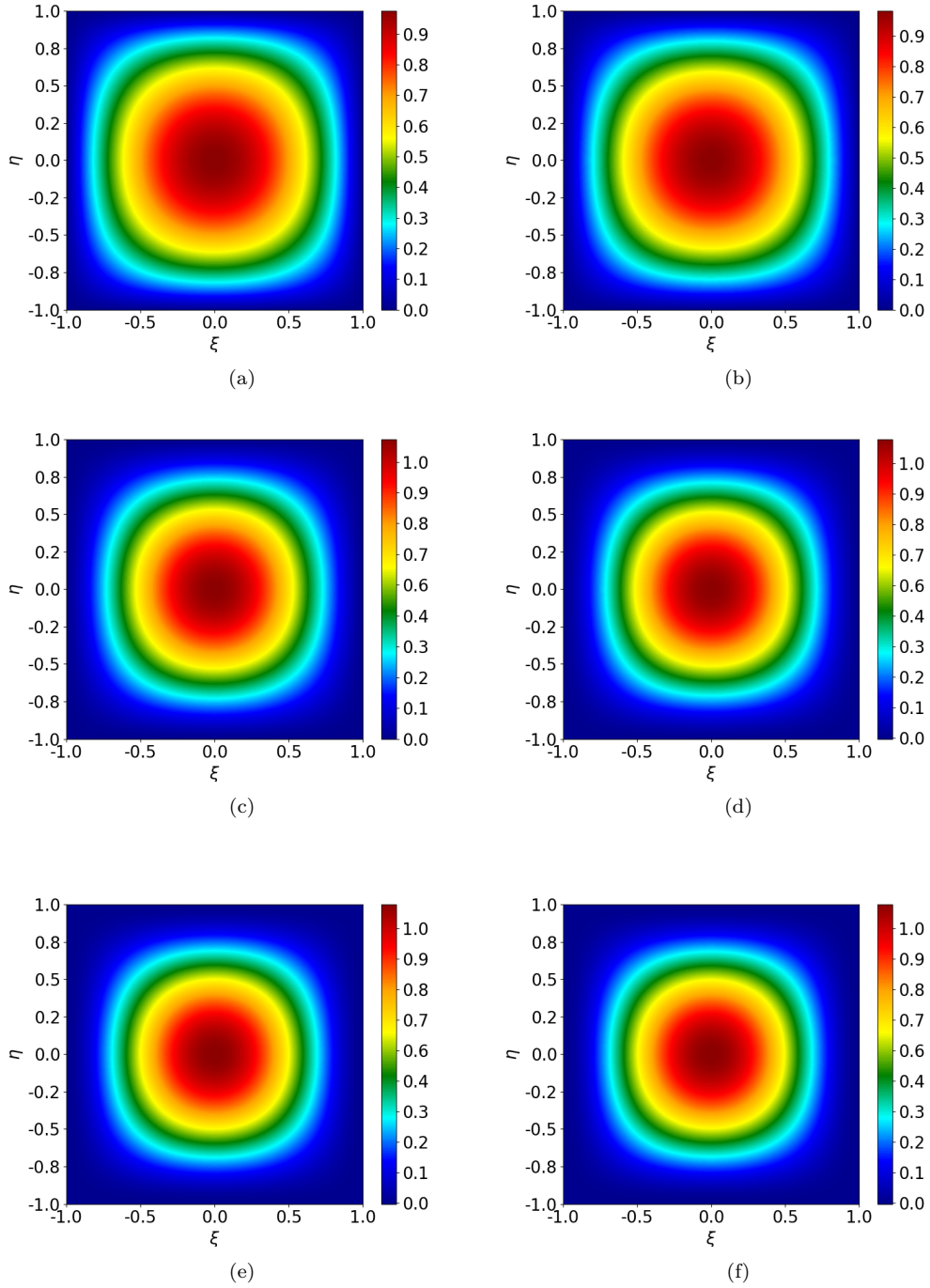


Figure 3: The first mode shape of a square isotropic plate with all four edges rotationally restrained: (a) $r_\xi = r_\eta = 0$; (b) $r_\xi = r_\eta = 1$; (c) $r_\xi = r_\eta = 10$; (d) $r_\xi = r_\eta = 20$; (e) $r_\xi = r_\eta = 100$; (f) $r_\xi = r_\eta = \infty$.

Table 4: The first six frequency parameters, $2a\Omega = 2a\sqrt[4]{\rho h\omega^2/D_{11}}$, of a square isotropic plate with all four edges rotationally restrained, where $k_{\xi=-1}^r = k_{\xi=1}^r = k_{\eta=-1}^r = k_{\eta=1}^r$.

r	Mode	$2a\Omega$					
		1	2	3	4	5	6
0.1	Mode number	(1,1)	(1,2)	(2,1)	(2,2)	(1,3)	(3,1)
	Ref.20	4.454	6.992	7.045	8.890	9.782	9.960
	Ref.31	4.465	7.039	7.039	8.897	9.945	9.945
	Present (Ω_x)	4.463	7.028	7.043	8.893	9.938	9.953
	Present (Ω_y)	4.463	7.043	7.028	8.893	9.953	9.938
	Present (Ω)	4.463	7.035	7.035	8.893	9.945	9.945
	Difference (%)	0.044	0.056	0.056	0.044	0.000	0.000
1	Mode number	(1,1)	(1,2)	(2,1)	(2,2)	(3,1)	(1,3)
	Ref.20	4.529	7.008	7.136	8.936	9.787	10.036
	Ref.31	4.637	7.155	7.155	8.991	10.029	10.030
	Present (Ω_x)	4.648	7.098	7.223	8.993	10.093	9.968
	Present (Ω_y)	4.648	7.223	7.098	8.993	9.968	10.098
	Present (Ω)	4.648	7.160	7.160	8.993	10.030	10.033
	Difference (%)	0.237	0.069	0.069	0.022	0.009	0.029
10	Mode number	(1,1)	(1,2)	(2,1)	(2,2)	(1,3)	(3,1)
	Ref.31	5.346	7.768	7.768	9.537	10.552	10.563
	Present (Ω_x)	5.413	7.718	7.953	9.598	10.448	10.782
	Present (Ω_y)	5.413	7.953	7.718	9.598	10.782	10.453
	Present (Ω)	5.413	7.835	7.835	9.598	10.615	10.618
	Difference (%)	1.253	0.862	0.862	0.639	0.597	0.520
100	Mode number	(1,1)	(1,2)	(2,1)	(2,2)	(1,3)	(3,1)
	Ref.20	5.895	8.326	8.422	10.167	10.957	11.297
	Ref.31	5.901	8.442	8.442	10.253	11.307	11.333
	Present (Ω_x)	5.913	8.428	8.473	10.258	11.293	11.373
	Present (Ω_y)	5.913	8.473	8.478	10.258	11.373	11.293
	Present (Ω)	5.913	8.450	8.450	10.258	11.333	11.333
	Difference (%)	0.203	0.094	0.094	0.048	0.229	0.000
1000	Mode number	(1,1)	(1,2)	(2,1)	(2,2)	(1,3)	(3,1)
	Ref.31	6.011	8.585	8.585	10.424	11.495	11.522
	Present (Ω_x)	5.988	8.553	8.553	10.388	11.463	11.478
	Present (Ω_y)	5.988	8.553	8.553	10.388	11.478	11.463
	Present (Ω)	5.988	8.553	8.553	10.388	11.470	11.470
	Difference (%)	0.382	0.372	0.372	0.345	0.217	0.451

390 fundamental frequency results for different length ratios (b/a), comparing
391 them with those reported in 31. The maximum observed difference is 0.8%
392 when $r_{\eta=-1} = 10$.

393 ~~In~~ Interestingly, in certain numerical calculations involving rotationally
394 restrained boundary conditions, the variables α_1 and α_2 may take complex
395 values rather than being purely real. Consequently, the mode shape coeffi-
396 cients A_1 , A_2 , B_1 , and B_2 become complex-valued, leading to \mathbf{R} and \mathbf{Q}^{-1}
397 being complex matrices. However, the mode shapes $\phi(\xi)$ and $\psi(\eta)$ remain
398 real-valued, and the dynamic stiffness matrix $\mathbf{K} = \mathbf{R}\mathbf{Q}^{-1}$ is a real symmetric
399 matrix. Thus, the frequency Ω can be obtained by solving \mathbf{K} using the refined
400 W-W algorithm provided in this study, which avoids solving the eigenvalue
401 equations in both the real and complex domains.

Table 5: Fundamental frequency parameter $2a\Omega = 2a\sqrt[4]{\rho h\omega^2/D_{11}}$ of rectangular or-
thotropic plates with three edges simply supported ($k_{\xi=-1}^r = k_{\xi=1}^r = k_{\eta=1}^r = 0$) and
the edge at $\eta = -1$ rotationally restrained.

b/a	$r_{\eta=-1}$	$2a\Omega$				
		Ref.31	Present (Ω)	Present (Ω_x)	Present (Ω_y)	Difference (%)
0.5	0	7.530	7.523	7.523	7.523	0.092
	1	7.690	7.700	7.588	7.813	0.130
	10	8.250	8.308	8.198	8.418	0.703
	∞	8.705	8.695	8.695	8.695	0.114
1.0	0	4.917	4.918	4.918	4.918	0.020
	1	4.954	4.960	4.933	4.988	0.121
	10	5.114	5.128	5.088	5.168	0.273
	∞	5.289	5.278	5.278	5.278	0.207
1.5	0	4.126	4.128	4.128	4.128	0.048
	1	4.139	4.138	4.128	4.148	0.024
	10	4.202	4.208	4.188	4.228	0.142
	∞	4.292	4.288	4.288	4.288	0.093

5. Conclusion

In this study, the dynamic stiffness matrix (DSM) based on the extended separation-of-variable (SOV) ~~type~~ solution has been developed for the vibration analysis of an orthotropic rectangular plate with general homogeneous boundary conditions.

Instead of solving highly nonlinear eigenvalue equations involved in the SOV methods, the extended SOV ~~type~~ solution is adopted to construct the dynamic stiffness matrices. Several novel techniques have proposed to solve the eigenvalue problem and mode shape computation. The challenge of determining the fully clamped frequencies using the ~~Wittrick-Williams~~ ~~(W-W)~~ Wittrick-Williams (W-W) algorithm is resolved by computing the frequencies under specific boundary conditions, such as simply supported, guided, or a combination of the two, whose closed-form expression can be easily derived using the SOV method.

Classical boundary conditions, such as guided, simply supported, clamped, and free edges, can be realized by setting the translational springs (~~$k_x^v k_x^v$~~) and rotational springs (~~$k_x^r k_x^r$~~) along the plate edges to either zero or infinity, as appropriate. Numerical experiments ~~have validated~~ validate the accuracy of this approach for these boundary conditions. The results shows that the SOV ~~type~~ solution can also be extended to handle ~~elastically-restrained~~ elastically-restrained boundary conditions. Despite certain approximations inherent in some ~~elastically-restrained~~ elastically-restrained cases, the maximum percentage error across all numerical experiments remains within 1.25%. This may occur because the SOV ~~type~~ solution used is derived from the weak-form governing equation, which is based on Rayleigh's principle.

~~Since the SOV type~~ The SOV solution $\phi(\xi)\psi(\eta)$ consists of only ~~a one~~ a one single term for each mode order, unlike the ~~infinite series expansions~~ sufficiently truncated Fourier series used in the ~~traditional DSM~~ DSM for each mode, each eigenvalue solution can be explicitly expressed. Therefore, dynamic stiffness matrices based on the SOV solution have the minimum matrix dimension compared to existing DSM methods. This suggests the potential for ~~obtaining more concise solutions~~ constructing lower-dimensional dynamic stiffness matrices for assembled plate structures ~~compared to traditional DSM methods~~ than those produced by existing DSM approaches.

Finally, the developments reported in this paper should find good application with researchers and practitioners interested in the vibration of generally-supported rectangular orthotropic plates.

439 Appendix A Integral parameters

440 The integral parameters I_1 , I_2 , I_3 , and I_4 are defined as follows:

$$\begin{aligned}
 I_1 &= \int_0^1 \psi^2 d\eta \\
 &= (B_1^2 + B_2^2 - B_3^2 + B_4^2) + \frac{-B_1^2 + B_2^2}{2\alpha_2} \sin(2\alpha_2) + \frac{B_3^2 + B_4^2}{2\beta_2} \sinh(2\beta_2) \\
 &\quad + \frac{4(\alpha_2 B_2 B_4 + \beta_2 B_1 B_3)}{\alpha_2^2 + \beta_2^2} \sin(\alpha_2) \cosh(\beta_2) \\
 &\quad + \frac{4(-\alpha_2 B_1 B_3 + \beta_2 B_2 B_4)}{\alpha_2^2 + \beta_2^2} \cos(\alpha_2) \sinh(\beta_2).
 \end{aligned}
 \tag{A.1}$$

$$\begin{aligned}
 I_2 &= \int_0^1 \left(\psi \frac{d^2 \psi}{d\eta^2} \right) d\eta \\
 &= (-\alpha_2^2 B_1^2 - \alpha_2^2 B_2^2 - \beta_2^2 B_3^2 + \beta_2^2 B_4^2) \\
 &\quad + \frac{\alpha_2(B_1^2 - B_2^2)}{2} \sin(2\alpha_2) + \frac{\beta_2(B_3^2 + B_4^2)}{2} \sinh(2\beta_2) \\
 &\quad + \frac{2(-\alpha_2^2 + \beta_2^2)(\alpha_2 B_2 B_4 + \beta_2 B_1 B_3)}{\alpha_2^2 + \beta_2^2} \sin(\alpha_2) \cosh(\beta_2) \\
 &\quad + \frac{2(-\alpha_2^2 + \beta_2^2)(-\alpha_2 B_1 B_3 + \beta_2 B_2 B_4)}{\alpha_2^2 + \beta_2^2} \cos(\alpha_2) \sinh(\beta_2).
 \end{aligned}
 \tag{A.2}$$

$$\begin{aligned}
 I_3 &= \int_0^1 \left(\frac{d\psi}{d\eta} \right)^2 d\eta \\
 &= \alpha_2^2 B_1^2 + \alpha_2^2 B_2^2 + \beta_2^2 B_3^2 - \beta_2^2 B_4^2 \\
 &\quad + \frac{\alpha_2(B_1^2 - B_2^2)}{2} \sin(2\alpha_2) + \frac{\beta_2(B_3^2 + B_4^2)}{2} \sinh(2\beta_2) \\
 &\quad + \frac{4\alpha_2\beta_2(\alpha_2 B_1 B_3 - \beta_2 B_2 B_4)}{\alpha_2^2 + \beta_2^2} \sin(\alpha_2) \cosh(\beta_2) \\
 &\quad + \frac{4\alpha_2\beta_2(\alpha_2 B_2 B_4 + \beta_2 B_1 B_3)}{\alpha_2^2 + \beta_2^2} \cos(\alpha_2) \sinh(\beta_2).
 \end{aligned}
 \tag{A.3}$$

$$\begin{aligned}
I_4 &= \int_0^1 \left(\frac{d^2\psi}{d\eta^2} \right)^2 d\eta \\
&= \left(\alpha_2^4 B_1^2 + \alpha_2^4 B_2^2 - \beta_2^4 B_3^2 + \beta_2^4 B_4^2 \right) \\
&\quad + \frac{\alpha_2^3 (-B_1^2 + B_2^2)}{2} \sin(2\alpha_2) + \frac{\beta_2^3 (B_3^2 + B_4^2)}{2} \sinh(2\beta_2) \\
&\quad + \frac{4\alpha_2^2 \beta_2^2 (-\alpha_2 B_2 B_4 - \beta_2 B_1 B_3)}{\alpha_2^2 + \beta_2^2} \sin(\alpha_2) \cosh(\beta_2) \\
&\quad + \frac{4\alpha_2^2 \beta_2^2 (\alpha_2 B_1 B_3 - \beta_2 B_2 B_4)}{\alpha_2^2 + \beta_2^2} \cos(\alpha_2) \sinh(\beta_2)
\end{aligned} \tag{A.4}$$

444 The integral parameters J_1 , J_2 , J_3 , and J_4 can be obtained by replacing B_1
445 to B_4 by A_1 to A_4 , respectively, and α_2 and β_2 by α_1 and β_1 , respectively.

446 References

- 447 [1] Banerjee, J., Papkov, S., Liu, X., Kennedy, D., 2015. Dynamic stiffness
448 matrix of a rectangular plate for the general case. *Journal of Sound and*
449 *Vibration* 342, 177–199. doi:10.1016/j.jsv.2014.12.031.
- 450 [2] Banerjee, J.R., 1997. Dynamic stiffness formulation for structural el-
451 ements: a general approach. *Computers & Structures* 63, 101–103.
452 doi:10.1016/S0045-7949(96)00326-4.
- 453 [3] Biancolini, M.E., Brutti, C., Reccia, L., 2005. Approximate solution for
454 free vibrations of thin orthotropic rectangular plates. *Journal of Sound*
455 *and Vibration* 288, 321–344. doi:10.1016/j.jsv.2005.01.005.
- 456 [4] Boscolo, M., Banerjee, J., 2011. Dynamic stiffness elements and their ap-
457 plications for plates using first order shear deformation theory. *Comput-*
458 *ers & Structures* 89, 395–410. doi:10.1016/j.compstruc.2010.11.005.
- 459 [5] Fazzolari, F., Boscolo, M., Banerjee, J., 2013. An exact dynamic stiffness
460 element using a higher order shear deformation theory for free vibration
461 analysis of composite plate assemblies. *Composite Structures* 96, 262–
462 278. doi:10.1016/j.compstruct.2012.08.033.
- 463 [6] Ghorbel, O., Casimir, J.B., Hammami, L., Tawfiq, I., Haddar, M., 2015.
464 Dynamic stiffness formulation for free orthotropic plates. *Journal of*
465 *Sound and Vibration* 346, 361–375. doi:10.1016/j.jsv.2015.02.020.

- 466 [7] Gorman, D.J., 2005. Free in-plane vibration analysis of rectangular
467 plates with elastic support normal to the boundaries. *Journal of Sound*
468 *and Vibration* 285, 941–966. doi:10.1016/j.jsv.2004.09.017.
- 469 [8] Han, F., Dan, D., Cheng, W., Zang, J., 2018. An improved wittrick-
470 williams algorithm for beam-type structures. *Composite Structures* 204,
471 560–566. doi:10.1016/j.compstruct.2018.07.108.
- 472 [9] Kantorovich, L.V., Krylov, V.I., 1958. *Approximate Methods of Higher*
473 *Analysis*. Interscience Publishers, New York.
- 474 [10] Kerr, A.D., 1968. An extension of the kantorovich method. *Quarterly*
475 *of Applied Mathematics* 26, 219–229. doi:10.1090/qam/99857.
- 476 [11] Khov, H., Li, W.L., Gibson, R.F., 2009. An accurate solution method
477 for the static and dynamic deflections of orthotropic plates with general
478 boundary conditions. *Composite Structures* 90, 474–481. doi:10.1016/
479 j.compstruct.2009.04.020.
- 480 [12] Laura, P.A., Saffell Jr, B.F., 1967. Study of small-amplitude vibrations
481 of clamped rectangular plates using polynomial approximations. *The*
482 *Journal of the Acoustical Society of America* 41, 836–839. doi:10.1121/
483 1.1910414.
- 484 [13] Leissa, A.W., 1973. The free vibration of rectangular plates. *Jour-*
485 *nal of Sound and Vibration* 31, 257–293. doi:10.1016/S0022-460X(73)
486 80371-2.
- 487 [14] Levy, M., 1899. Sur l’équilibre élastique d’une plaque rectangulaire.
488 *Comptes Rendus Acad. Sci. Paris* 129, 535–539.
- 489 [15] Li, R., Zhong, Y., Tian, B., Liu, Y., 2009a. On the finite integral trans-
490 form method for exact bending solutions of fully clamped orthotropic
491 rectangular thin plates. *Applied Mathematics Letters* 22, 1821–1827.
492 doi:10.1016/j.aml.2009.07.003.
- 493 [16] Li, W.L., 2004. Vibration analysis of rectangular plates with general
494 elastic boundary supports. *Journal of Sound and Vibration* 273, 619–
495 635. doi:10.1016/S0022-460X(03)00562-5.

- 496 [17] Li, W.L., Zhang, X., Du, J., Liu, Z., 2009b. An exact series solu-
497 tion for the transverse vibration of rectangular plates with general elas-
498 tic boundary supports. *Journal of Sound and Vibration* 321, 254–269.
499 doi:10.1016/j.jsv.2008.09.035.
- 500 [18] Liu, X., Banerjee, J., 2015. An exact spectral-dynamic stiffness
501 method for free flexural vibration analysis of orthotropic composite
502 plate assemblies—part i: Theory. *Composite Structures* 132, 1274–1287.
503 doi:10.1016/j.compstruct.2015.07.020.
- 504 [19] Liu, X., Banerjee, J., 2016. Free vibration analysis for plates with
505 arbitrary boundary conditions using a novel spectral-dynamic stiff-
506 ness method. *Computers & Structures* 164, 108–126. doi:10.1016/
507 j.compstruc.2015.11.005.
- 508 [20] Mukhopadhyay, M., 1979. Free vibration of rectangular plates with
509 edges having different degrees of rotational restraint. *Journal of Sound*
510 *and Vibration* 67, 459–468.
- 511 [21] Navier, L., 1823. Extrait des recherches sur la flexion des plans elas-
512 tiques. *Bull. Sci. Soc. Philomat.* , 95–102.
- 513 [22] Timoshenko, S., 1940. *Theory of Plates and Shells*. McGraw-Hill Book
514 Company.
- 515 [23] Wittrick, W.H., Williams, F.W., 1971. A general algorithm for comput-
516 ing natural frequencies of elastic structures. *The Quarterly Journal of*
517 *Mechanics and Applied Mathematics* 24, 263–284. doi:10.1093/qjmam/
518 24.3.263.
- 519 [24] Xing, Y., Li, G., Yuan, Y., 2022. A review of the analytical solution
520 methods for the eigenvalue problems of rectangular plates. *International*
521 *Journal of Mechanical Sciences* 221, 107171. doi:10.1016/j.ijmecsci.
522 2022.107171.
- 523 [25] Xing, Y., Liu, B., 2009a. New exact solutions for free vibrations of
524 rectangular thin plates by symplectic dual method. *Acta Mechanica*
525 *Sinica* 25, 265–270. doi:10.1007/s10409-008-0208-4.
- 526 [26] Xing, Y., Sun, Q., Liu, B., Wang, Z., 2018. The overall assessment
527 of closed-form solution methods for free vibrations of rectangular thin

- 528 plates. International Journal of Mechanical Sciences 140, 455–470.
529 doi:10.1016/j.ijmecsci.2018.03.013.
- 530 [27] Xing, Y., Wang, Z., 2020a. An extended separation-of-variable method
531 for the free vibration of orthotropic rectangular thin plates. International
532 Journal of Mechanical Sciences 182, 105739. doi:10.1016/j.ijmecsci.
533 2020.105739.
- 534 [28] Xing, Y., Wang, Z., 2020b. An improved separation-of-variable method
535 for the free vibration of orthotropic rectangular thin plates. Composite
536 Structures 252, 112664. doi:10.1016/j.compstruct.2020.112664.
- 537 [29] Xing, Y.F., Liu, B., 2009b. New exact solutions for free vibrations of
538 thin orthotropic rectangular plates. Composite Structures 89, 567–574.
539 doi:10.1016/j.compstruct.2008.11.010.
- 540 [30] Yuan, S., Ye, K., Williams, F., 2004. Second order mode-finding method
541 in dynamic stiffness matrix methods. Journal of Sound and Vibration
542 269, 689–708. doi:10.1016/S0022-460X(03)00126-3.
- 543 [31] Zhang, S., Xu, L., Li, R., 2019. New exact series solutions for transverse
544 vibration of rotationally-restrained orthotropic plates. Applied Mathe-
545 matical Modelling 65, 348–360. doi:10.1016/j.apm.2018.08.033.
- 546 [32] Zhong, W.X., 1995. A new systematic methodology for theory of elas-
547 ticity. Dalian University of Technology Press, Dalian , 182–187.
- 548 [33] Zhong, Y., Zhao, X.F., Li, R., 2013. Free vibration analysis of rectangu-
549 lar cantilever plates by finite integral transform method. International
550 Journal for Computational Methods in Engineering Science and Me-
551 chanics 14, 221–226. doi:10.1080/15502287.2012.711424.